TABLE 1. Candidate HLA-A*0201-restricted T-cell epitopes in the p51-70 peptide of the MPT51 molecule

Peptide[a]	Amino acid sequence[b]	Estimated scores for restriction molecules	
		BIMAS	SYFPEITHI
p51-70	MNTLAGKGISVVAPA GGAYS		
Nonamers			
p53-61	**TLAGKGISV**	69.552	27
p54-62	LAGKGISVV	1.549	22
Decamers			
p53-62	**TLAGKGISVV**	65.588	28
p50-59	AMNTLAGKGI	7.535	19
p52-61	NTLAGKGISV	3.574	18

[a] Data for peptides ranked in the top 20 in the BIMAS or SYFPEITHI algorithms are shown.

[b] Boldface type indicates peptide sequences that were synthesized and used for experiments. Underlining indicates anchor residues. The G residues in p53-62 are residues that are associated with good binding to A*0201, as suggested by Ruppert et al. (28).

washed twice with RPMI 1640 medium, and resuspended in RPMI/10FCS. For some experiments, peripheral blood mononuclear cells (PBMCs) from purified protein derivative (PPD)-reactive HLA-A*0201$^+$ human healthy subjects were prepared by LeucoSep (Greiner Bio-One, Frickenhausen, Germany) according to the manufacturer's instructions. These cells (1×10^6 cells) were washed twice with FACS buffer and stained with the PE-labeled HLA-A*0201/MPT51 p53-62 tetramer and FITC-labeled anti-mouse or -human CD8 MAb for 30 min at 4°C. The cells were then washed with FACS buffer twice and analyzed with a digital flow cytometer (EPICS XL; Beckman Coulter).

RESULTS

IFN-γ production in response to overlapping synthetic peptides from MPT51 in HHD mice. Splenocytes from HHD mice immunized with a DNA vaccine encoding mature MPT51 (pCI-MPT51) were stimulated with the overlapping MPT51 peptides for 24 h, and the IFN-γ concentrations in culture supernatants were determined by ELISA. As shown in Fig. 1, robust IFN-γ production was observed in splenocytes from MPT51 DNA-vaccinated HHD mice after stimulation with peptide 51 (p51) (amino acid residues 51 to 70) and peptide 171 (p171) (amino acid residues 171 to 190). In addition, weak IFN-γ production was observed in the splenocytes in the presence of peptide 191 (p191) (amino acid residues 191 to 210). Since the HHD mice that we used in this study had a C57BL/6 background (25) and we observed that only CD4$^+$ T cells produced IFN-γ in response to p171 and p191, we concluded that CD4$^+$ T cells responded to these peptides presented on H2-A^b molecules and produced IFN-γ (34). As expected, spleen cells from naïve HHD mice showed no significant IFN-γ production in response to any MPT51 peptide.

Identification of a 10-mer CD8$^+$ T-cell epitope in peptide p51-70 of MPT51. Since CD8$^+$ T-cell epitopes presented by MHC class I molecules comprise 8 to 10 amino acids and are generally 9 amino acids long, we pursued a line of inquiry to identify the fine HLA-A*0201-restricted CD8$^+$ T-cell epitope. We predicted candidate peptides in the 20-mer peptide by using the computer-based programs BIMAS HLA Peptide Binding Predictions and SYFPEITHI Epitope Prediction. Using the BIMAS program, we found that a 9-mer peptide, p53-61 (TLAGKGISV), and a 10-mer peptide, p53-62 (TLAGKGISVV), showed high scores for binding to the HLA-A*0201 molecule in the region containing amino acid residues 51 to 70 (the binding scores were 69.552 for p53-61 and 65.588 for p53-62) (Table 1). In addition, the SYFPEITHI program also produced high scores for these peptides (27 for p53-61 and 28 for p53-62) (Table 1). Therefore, we synthesized p53-61 (TLAGKGISV) and p53-62 (TLAGKGISVV). In addition, we synthesized the p21-29 peptide (FLAGGPHAV) since this peptide had the highest HLA-A*0201 binding scores with the BIMAS and SYFPEITHI programs (319.939 and 29, respectively). Three-color flow cytometric analysis showed that the number of IFN-γ-producing CD8$^+$ T cells increased in the

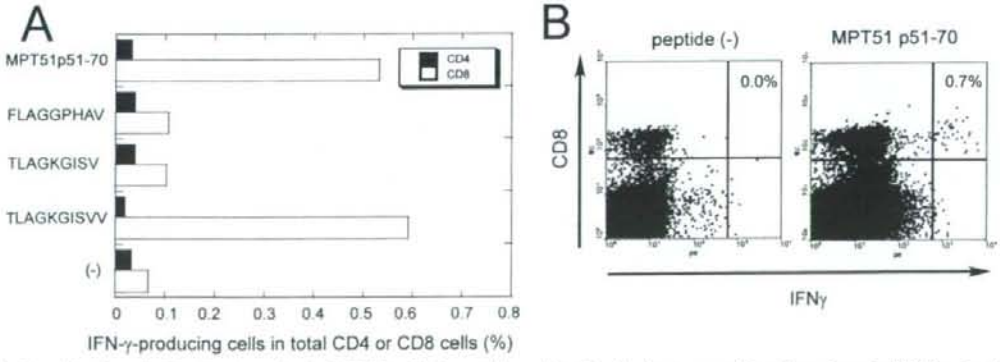

FIG. 2. Identification of a T-cell epitope in the MPT51 p53-62 peptide and the T-cell subset recognizing the epitope in HHD mice. (A) Levels of IFN-γ-producing T-cell subsets in spleens of HHD mice immunized with the pCI-MPT51 plasmid. Three-color flow cytometric analysis was performed for detection of intracellular IFN-γ and cell surface CD4 and CD8 molecules after immune splenocytes were cultured in the presence of the MPT51-derived peptides p51-70 (20-mer peptide), p21-29 (FLAGGPHAV), p53-61 (TLAGKGISV), and p53-62 (TLAGKGISVV). The data are the percentages of IFN-γ-producing CD4$^+$ or CD8$^+$ cells in the total CD4$^+$ or CD8$^+$ cells after 4 h of stimulation with peptides. The results of a representative experiment are shown. (B) Representative flow cytometry data for intracellular IFN-γ and cell surface CD8 staining of spleen cells of HHD mice immunized with the pCI-MPT51 plasmid after 4 h of stimulation with the MPT51 p51-70 peptide. The percentages of IFN-γ-producing cells in the total CD8$^+$ cells are shown.

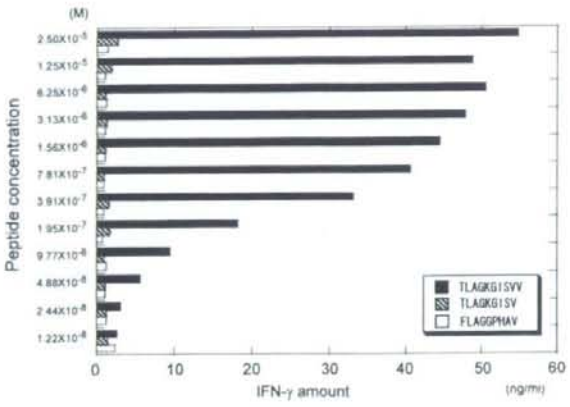

FIG. 3. MPT51 p53-62 is a dominant T-cell epitope in HHD mice. The IFN-γ production by splenocytes from HHD mice immunized with the pCI-MPT51 plasmid in response to twofold serially diluted doses of candidate peptides MPT51 p53-62 (TLAGKGISVV), p53-61 (TLAGKGISV), and p21-29 (FLAGGPHAV) was evaluated. The data are representative of the results of three independent experiments.

presence of p53-62 (TLAGKGISVV) but not in the presence of p53-61 (TLAGKGISV) or p21-29 (FLAGGPHAV) (Fig. 2). The MPT51 p53-62 peptide was confirmed to stimulate splenocytes derived from MPT51 DNA-immune HHD mice in a dose-dependent manner. The minimum concentration of this peptide for inducing IFN-γ production by the splenocytes was approximately 5×10^{-8} M (50 nM) (Fig. 3).

Binding affinity of the p53-62 peptide to the HLA-A*0201 molecule. We then examined the binding affinity of the MPT51 p53-62 peptide to the HLA-A*0201 molecule by measuring the binding stability with T2 cells, and we compared this peptide with several other *M. tuberculosis*-derived epitopes in terms of binding stability. T2 cells are defective for endogenous class I presentation due to the TAP deficiency, but peptide loading on MHC molecules stabilizes the expression of MHC on the cell surface (33). The MHC molecules stabilized with the appropriate peptides could be detected by flow cytometry with an MAb to the HLA-A*0201 molecule. As shown in Fig. 4A, MPT51 p21-29 (FLAGGPHAV) and MPT51 p53-62 (TLAG KGISVV) were strongly bound to the HLA-A*0201 molecule on T2 cells, whereas MPT51 p53-61 (TLAGKGISV), a known *M. tuberculosis* Ag85A-derived HLA-A*0201-binding peptide (KLIANNTRV) (30), and an *M. tuberculosis* ESAT6-derived HLA-A*0201-binding peptide (LLDEGKQSL) (19) were relatively weakly bound to the HLA-A*0201 molecule.

To obtain insight into T-cell recognition of the MPT51 p53-62/HLA-A*0201 complex on T2 cells, we examined the cytotoxic T-cell response of immune mice to the peptide-MHC complex. As shown in Fig. 4B, immune splenocytes of MPT51 DNA-immune HHD mice after in vitro stimulation with MPT51 p53-62 peptide-pulsed autologous splenocytes lysed the peptide-pulsed T2 cells substantially. However, the immune splenocytes did not lyse MPT51 p21-29 peptide-pulsed T2 cells after in vitro stimulation with the peptide-pulsed autologous splenocytes (Fig. 4A), although the peptide bound relatively strongly to HLA-A*0201 on T2 cells (data not shown).

Detection of MPT51 p53-62-specific $CD8^+$ T cells in PBMCs of HLA-A*0201$^+$ PPD-reactive healthy subjects. Finally, we examined whether HLA-A*0201$^+$ PPD-reactive healthy subjects do have MPT51 p53-62-specific memory T cells. We screened PBMCs of HLA-A*0201$^+$ individuals for the presence of the memory T cells. HLA-A*0201$^+$ PPD-reactive PBMCs were subjected to MPT51 p53-62/HLA-A*0201 tetramer staining after in vitro stimulation with mitomycin C-treated, MPT51 p53-62-pulsed autologous PBMCs for 10 days. As shown in Fig. 5A, PBMCs from some HLA-A*0201-positive PPD-reactive individuals showed larger amounts of MPT51 p53-62/HLA-A*0201 tetramer-positive $CD8^+$ T cells by flow cytometric analysis than PBMCs from HLA-A*0201-negative individuals. The PBMCs of two of five HLA-A*0201-positive individuals were tetramer positive. In parallel, the

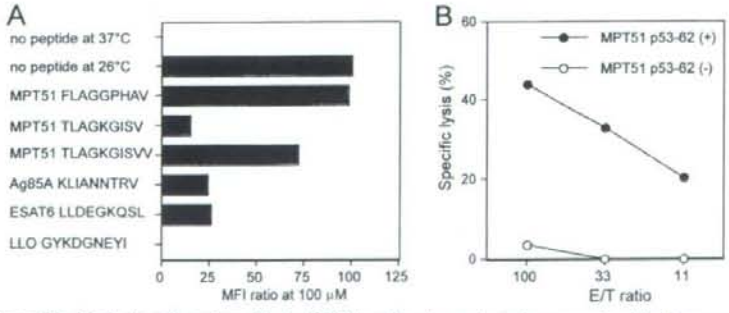

FIG. 4. MPT51 p53-62 peptide binds to cell surface HLA-A*0201 molecules and can be recognized by immune T cells in the context of HLA-A*0201. (A) HLA binding assay with T2 cells showing that MPT51 p21-29 (FLAGGPHAV) and MPT51 p53-62 (TLAGKGISVV) bound to HLA-A*0201 strongly, whereas MPT51 p53-61 (TLAGKGISV), the Ag85A-derived peptide KLIANNTRV, and the ESAT6-derived peptide LLDEGKQSL bound to HLA-A*0201 relatively weakly. The MFI ratios in the presence of the indicated peptides at a concentration of 100 μM are shown. The listeriolysin O (LLO)-derived peptide GYKDGNEYI was used as a negative control. The expression of HLA-A*0201 on T2 cells cultured in the absence of any peptide at 37 or 26°C is also shown. Representative data from three independent experiments are shown. (B) Lysis of MPT51 p53-62 peptide-pulsed T2 cells by splenocytes from MPT51 DNA-immune HHD mice. Immune splenocytes (effectors) were incubated with target cells using the effector/target cell ratios (E/T ratio) indicated on the *x* axis. Representative data from three independent experiments are shown.

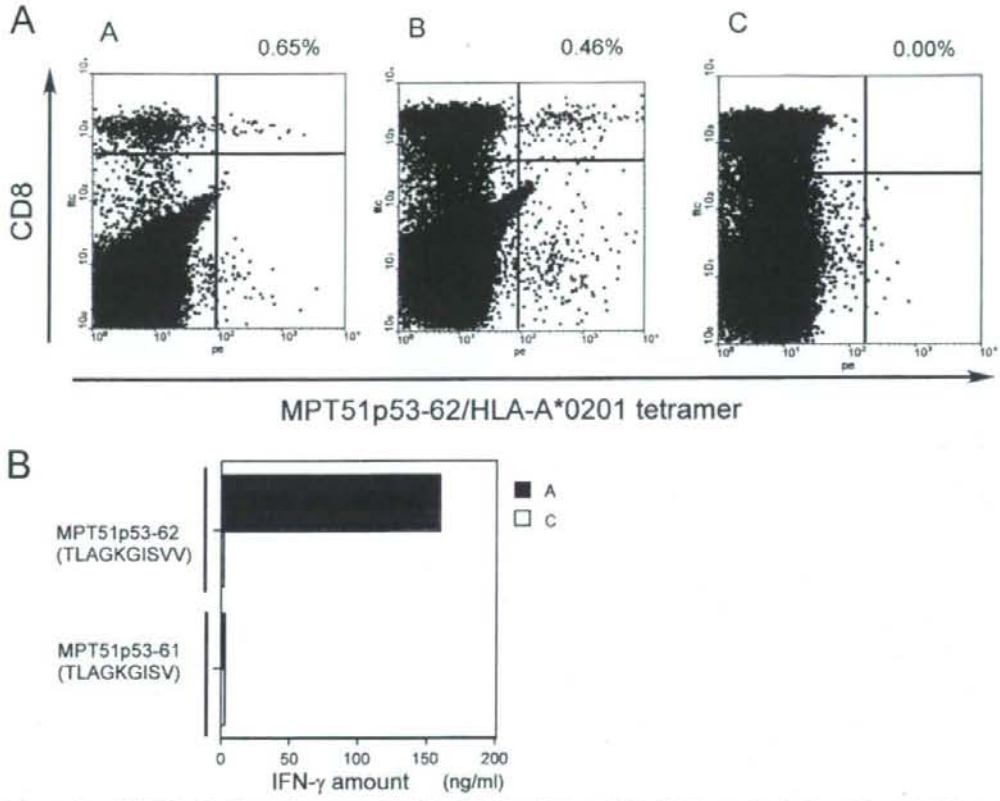

FIG. 5. Detection of MPT51 p53-62-specific memory T cells in PBMCs of HLA-A*0201$^+$ PPD-reactive healthy subjects. (A) Flow cytometric analyses to detect MPT51 p53-62-specific memory T cells in PBMCs of HLA-A*0201$^+$ PPD-reactive healthy subjects using MPT51 p53-62/HLA-A*0201 tetramer. PBMCs of the healthy subjects were prepared and cultured for 10 days together with mitomycin C-treated, MPT51 p53-62-pulsed autologous PBMCs and then subjected to flow cytometric analysis after treatment with PE-conjugated MPT51 p53-62/HLA-A*0201 tetramer and FITC-conjugated anti-human CD8 MAb staining (graphs A and B). HLA-unmatched PBMCs were used as a negative control (graph C). Representative flow cytometry patterns are shown. The percentages of tetramer-positive cells in the total CD8$^+$ cells are indicated. (B) IFN-γ production by PBMCs of HLA-A*0201$^+$ PPD-reactive healthy subjects stimulated with MPT51 p53-62 (TLAGKGISVV)- or p53-61 (TLAGKGISV)-pulsed autologous PBMCs for 10 days as evaluated by an IFN-γ ELISA. Samples A and C correspond to graphs A and C in panel A.

tetramer-positive PBMCs produced large amounts of IFN-γ after in vitro stimulation (Fig. 5B).

DISCUSSION

Here we identified induction of an MPT51 p53-62/HLA-A*0201-specific T-cell population by using HLA-A*0201 transgenic mice (HHD mice) and the MPT51 expression plasmid pCI-MPT51. From the data described above, we were able to draw the following conclusions about a T-cell epitope on the mature MPT51 molecule of *M. tuberculosis*: (i) MPT51 p53-62 peptide is a bona fide HLA-A*0201-restricted CD8$^+$ T-cell epitope and (ii) epitope-specific memory T cells were detected in PBMCs of HLA-A*0201-positive PPD-reactive healthy subjects.

A greater understanding of the nature of protective immunity to *M. tuberculosis* would facilitate development of a vaccine. The cellular arm of the immune response mediated by CD4$^+$ Th1 and CD8$^+$ CTL has been determined to be a pivotal component of protective immunity against *M. tuberculosis* (17). IFN-γ secretion, cytotoxic ability, and direct killing of *M. tuberculosis* by CD8$^+$ T cells have been speculated to be involved in protection (18). We report here that an MPT51 p53-62 peptide/HLA-A*0201 complex can be recognized by CD8$^+$ T cells producing IFN-γ and exhibiting CTL activity.

Reports concerning the involvement of CD8$^+$ T cells in containing *M. tuberculosis* infection in human have been accumulating, and intense efforts have been made to identify *M. tuberculosis*-derived CD8$^+$ T-cell epitopes that can be presented by HLA class I molecules. *M. tuberculosis*-derived HLA-A*0201-restricted T-cell epitopes have been identified, including epitopes in Ag85A (30), ESAT-6 (19), Ag85B (14), heat shock protein 65 (7), the 16-kDa protein (6), the 28-kDa protein (8), the 38-kDa protein (8), superoxide dismutase (9), alanine dehydrogenase (9), glutamine synthetase (9), the 19-kDa protein (21), and Rv0341 (12).

MPT51 is a dominant *M. tuberculosis*-derived secreted molecule which is related to the Ag85 family molecules Ag85A,

Ag85B, and Ag85C. Such molecules have been found in a variety of mycobacteria (22). Functionally, these molecules have been implicated in fibronectin binding, like Ag85 family molecules (1). However, MPT51 appears not to have mycolyltransferase activity, which Ag85 family molecules have, since MPT51 does not have the catalytic triad (Ser-His-Glu) in its amino acid sequence (36). Therefore, MPT51 seems to have a function that remains to be clarified. Importantly, MPT51 has been reported to be a potential marker for the diagnosis of TB, especially in AIDS patients. Ramalingam and colleagues (26) reported that early immune responses against 38- and 27-kDa (MPT51) proteins were detected in pulmonary TB patients, accompanied by human immunodeficiency virus coinfection. In addition, we demonstrated that MPT51 DNA vaccination using an attenuated *Listeria* carrier vaccination system induced protection against *M. tuberculosis* infection in mice (20).

HLA transgenic mice have been widely used for detection of HLA-restricted T-cell epitopes. In this study we used HHD mice. In HHD mice, the HLA-A*0201 monochain is the only type of MHC class I molecule expressed (25). Firat and colleagues (11) reported that not only the size but also the diversity of the $CD8^+$ T-cell receptor repertoire is substantially larger in HHD mice than in $A*0201/K^b$ transgenic mice, which still express mouse $H2^b$ class I molecules. In addition, we used the computer algorithm programs BIMAS and SYFPEITHI for epitope prediction. These programs were helpful for narrowing down the amino acid region of the bona fide T-cell epitope.

HLA-A*0201-restricted $CD8^+$ T-cell epitopes have been identified in a variety of antigens, including antigens derived from cancers, viruses, bacteria, and protozoans. The main anchor amino acid positions are position 2 (Leu) and position 9 (Val), which were conserved in MPT51 p53-62 (TLAGKGIS VV). Most HLA-A*0201-restricted T-cell epitopes were nonamer peptides (10, 24), but some epitopes were decamer peptides, such as influenza virus matrix protein p59-68 (15). It is shown here that the MPT51 p53-62 decamer peptide was capable of binding to HLA-A*0201 and stimulating $CD8^+$ T cells of immune HHD mice, but the MPT51 p53-61 nonamer was not able to do these things. The conformational and electrostatic differences between the nonamer and the decamer should affect their binding affinity to the HLA-A*0201 molecule and subsequent T-cell responses. Ruppert and colleagues (28) studied in detail the roles of different amino acid residues at each position of nonamer or decamer peptides for binding to the HLA-A*0201 molecule. They suggested that the nonamer and decamer peptides have different preferences for amino acid residues for binding to the HLA-A*0201 molecule. For example, they showed that Tyr, Phe, and Trp residues at positions 1, 3, and 5 in nonamer peptides and Gly residues at positions 4 and 6 in decamer peptides are preferred for binding to HLA-A*0201. According to the speculation of these workers, the MPT51 p53-62 peptide seems to have better A*0201 binding features than the MPT51 p53-61 peptide (Gly residues at positions 4 and 6 in the MPT51 p53-62 peptide are suggested to be associated with good A*0201 binding) (Table 1). Interestingly, the MPT51 p21-29 peptide (FLAGGPHAV) was not immunogenic in terms of IFN-γ production and CTL ability, although this peptide showed high affinity to HLA-A*0201 (Fig. 4A), as predicted by MHC binding algorithms. Previous reports showed that there is a strong association between immunodominance and HLA binding affinity (13). But the results described here suggest that binding of peptides to the restricted MHC molecules is a prerequisite for T-cell epitopes; however, not all the peptides which show high-affinity binding for MHC molecules are necessarily immunodominant epitopes.

When we examined HLA-A*0201$^+$ PPD-reactive PBMCs for the response against MPT51 p53-62, we observed the specific $CD8^+$ T-cell response in some individuals. However, we could not detect $CD8^+$ T-cell responses in HLA-matched subjects without in vitro stimulation with the peptide. Therefore, we cannot rule out the possibility that these T cells were primed in vitro during stimulation with the peptide. The frequency of the memory T cells and the kinetics after *M. tuberculosis* infection are important issues to be clarified in the future.

In conclusion, we identified one HLA-A*0201-restricted $CD8^+$ CTL epitope on MPT51 in HHD mice, which may play a pivotal role in protection against *M. tuberculosis* infection. The identification of T-cell epitopes should be very useful for further elucidating the role of MPT51-specific T cells in protective immunity using tetramer staining or intracellular cytokine staining and also for future vaccine design.

ACKNOWLEDGMENTS

This work was supported by grants-in-aid for scientific research from the Japanese Society for the Promotion of Science (grant 11670260 to T.N. and grant 13670268 to Y.K.), by a grant-in-aid for the Centers of Excellence research program from the Ministry of Education, Culture, Sports, Science and Technology of Japan, by a Health and Labor Science Research Grant for Research on Emerging and Re-emerging Infectious Diseases from the Ministry of Health, Labor and Welfare of Japan, and by a grant-in-aid from the United States-Japan Cooperative Medical Science Program.

We thank the NIH Tetramer Facility for providing the HLA-A*0201-peptide tetramer complex, P. Creswell (Yale University School of Medicine) for providing the TAP-deficient T2 cell line, and F. A. Lemonnier (Pasteur Institute) for providing the HLA-A*0201 transgenic HHD mice. The technical assistance of K. Shibata (Hamamatsu University School of Medicine) with the flow cytometric analysis is gratefully acknowledged.

REFERENCES

1. **Abou-Zeid, C., T. L. Ratliff, H. G. Wiker, M. Harboe, J. Bennedsen, and G. A. W. Rook.** 1988. Characterization of fibronectin-binding antigens released by *Mycobacterium tuberculosis* and *Mycobacterium bovis* BCG. Infect. Immun. **56:**3046–3051.
2. **Andersen, P.** 1994. Effective vaccination of mice against *Mycobacterium tuberculosis* infection with a soluble mixture of secreted mycobacterial proteins. Infect. Immun. **62:**2536–2544.
3. **Andersen, P., Å. B. Andersen, A. L. Sørensen, and S. Nagai.** 1995. Recall of long-lived immunity to *Mycobacterium tuberculosis* infection in mice. J. Immunol. **154:**3359–3372.
4. **Baldwin, S. L., C. d'Souza, A. D. Roberts, B. P. Kelly, A. A. Frank, M. A. Lui, J. B. Ulmer, K. Huygen, D. M. McMurray, and I. A. Orme.** 1998. Evaluation of new vaccines in the mouse and guinea pig model of tuberculosis. Infect. Immun. **66:**2951–2959.
5. **Belisle, J. T., V. D. Vissa, T. Sievert, K. Takayama, P. J. Brennan, and G. S. Besra.** 1997. Role of the major antigen of *Mycobacterium tuberculosis* in cell wall biogenesis. Science **276:**1420–1422.
6. **Caccamo, N., S. Milano, C. Di Sano, D. Cigna, J. Ivanyi, A. M. Krensky, F. Dieli, and A. Salerno.** 2002. Identification of epitopes of *Mycobacterium tuberculosis* 16-kDa protein recognized by human leukocyte antigen-A*0201 $CD8^+$ T lymphocytes. J. Infect. Dis. **186:**991–998.
7. **Charo, J., A. Geluk, M. Sundbäck, B. Mirzai, A. D. Diehl, K.-J. Malmberg, A. Achour, S. Huriguchi, K. E. van Meijgaarden, J.-W. Drijfhout, N. Beekman, P. van Veelen, F. Ossendorp, T. H. M. Ottenhoff, and R. Kiessling.** 2001. The identification of a common pathogen-specific HLA class I A*0201-

restricted cytotoxic T cell epitope encoded within the heat shock protein 65. Eur. J. Immunol. **31**:3602–3611.

8. **Cho, S., V. Mehra, S. Thoma-Uszynski, S. Stenger, N. Serbina, R. J. Mazzaccaro, J. L. Flynn, P. F. Barnes, S. Southwood, E. Celis, B. R. Bloom, R. L. Modlin, and A. Sette.** 2000. Antimicrobial activity of MHC class I-restricted CD8$^+$ T cells in human tuberculosis. Proc. Natl. Acad. Sci. USA **97**:12210–12215.
9. **Dong, Y., S. Demaria, X. Sun, F. R. Santoni, B. M. Jesdale, A. S. De Groot, W. N. Rom, and Y. Bushkin.** 2004. HLA-A2-restricted CD8$^+$-cytotoxic-T-cell responses to novel epitopes in *Mycobacterium tuberculosis* superoxide dismutase, alanine dehydrogenase, and glutamine synthetase. Infect. Immun. **72**:2412–2415.
10. **Falk, K., O. Rötzschke, S. Stevanović, G. Jung, and H. G. Rammensee.** 1991. Allele-specific motifs revealed by sequencing of self-peptides eluted from MHC molecules. Nature **351**:290–296.
11. **Firat, H., M. Cochet, P. S. Rohrlich, F. Garcia-Pons, S. Darche, O. Danos, F. A. Lemonnier, and P. Langlade-Demoyen.** 2002. Comparative analysis of the CD8$^+$ T cell repertoires of H-2 class I wild-type/HLA-A2.1 and H-2 class I knockout/HLA-A2.1 transgenic mice. Int. Immunol. **14**:925–934.
12. **Flyer, D. C., V. Ramakrishna, C. Miller, H. Myers, M. McDaniel, K. Root, C. Flournoy, V. H. Engelhard, D. H. Canaday, J. A. Marto, M. M. Ross, D. F. Hunt, J. Shabanowitz, and F. M. White.** 2002. Identification by mass spectrometry of CD8$^+$-T-cell *Mycobacterium tuberculosis* epitopes within the Rv0341 gene product. Infect. Immun. **70**:2926–2932.
13. **Geluk, A., V. Taneja, K. E. van Meijgaarden, E. Zanelli, C. Abou-Zeid, J. E. R. Thole, R. R. P. de Vries, C. S. David, and T. H. M. Ottenhoff.** 1998. Identification of HLA class II-restricted determinants of *Mycobacterium tuberculosis*-derived proteins by using HLA-transgenic, class II-deficient mice. Proc. Natl. Acad. Sci. USA **95**:10797–10802.
14. **Geluk, A., K. E. van Meijgaarden, K. L. M. C. Franken, J. W. Drijfhout, S. D'Souza, A. Necker, K. Huygen, and T. H. M. Ottenhoff.** 2000. Identification of major epitopes of *Mycobacterium tuberculosis* AG85B that are recognized by HLA-A*0201-restricted CD8$^+$ T cells in HLA-transgenic mice and humans. J. Immunol. **165**:6463–6471.
15. **Gotch, F., A. McMichael, and J. Rothbard.** 1988. Recognition of influenza A matrix protein by HLA-A2-restricted cytotoxic T lymphocytes. J. Exp. Med. **168**:2045–2057.
16. **Kaufmann, S. H. E.** 2000. Is the development of a new tuberculosis vaccine possible? Nat. Med. **6**:955–960.
17. **Kaufmann, S. H. E.** 2003. Immunity to intracellular bacteria, p. 1229–1261. *In* W. E. Paul (ed.), Fundamental immunology, 5th ed. Lippincott Williams & Wilkins Publishers, Philadelphia, PA.
18. **Kaufumann, S. H. E., and J. L. Flynn.** 2005. CD8 T cells in tuberculosis, p. 465–474. *In* S. T. Cole, K. D. Eisenach, D. N. McMurray, and W. R. Jacobs, Jr. (ed.), Tuberculosis and the tubercle bacillus. ASM Press, Washington, DC.
19. **Lalvani, A., R. Brookes, R. J. Wilkinson, A. S. Malin, A. A. Pathan, P. Andersen, H. Dockrell, G. Pasvol, and A. V. S. Hill.** 1998. Human cytolytic and interferon γ-secreting CD8$^+$ T lymphocytes specific for *Mycobacterium tuberculosis*. Proc. Natl. Acad. Sci. USA **95**:270–275.
20. **Miki, K., T. Nagata, T. Tanaka, Y.-H. Kim, M. Uchijima, N. Ohara, S. Nakamura, M. Okada, and Y. Koide.** 2004. Induction of protective cellular immunity against *Mycobacterium tuberculosis* by recombinant attenuated self-destructing *Listeria monocytogenes* strains harboring eukaryotic expression plasmids for antigen 85 complex and MPB/MPT51. Infect. Immun. **72**:2014–2021.
21. **Mohagheghpour, N., D. Gammon, L. M. Kawamura, A. van Vollenhoven, C. J. Benike, and E. G. Engleman.** 1998. CTL response to *Mycobacterium tuberculosis*: identification of an immunogenic epitope in the 19-kDa lipoprotein. J. Immunol. **161**:2400–2406.
22. **Ohara, N., H. Kitaura, H. Hotokezaka, T. Nishiyama, N. Wada, S. Matsumoto, T. Matsuo, M. Naito, and T. Yamada.** 1995. Characterization of the gene encoding the MPB51, one of the major secreted protein antigens of *Mycobacterium bovis* BCG, and identification of the secreted protein closely related to the fibronectin binding 85 complex. Scand. J. Immunol. **41**:433–442.
23. **Pablos-Méndez, A., M. C. Raviglione, A. Laszlo, N. Binkin, H. L. Rieder, F. Bustreo, D. L. Cohn, C. S. B. Lanbregts-van Weezenbeek, S. J. Kim, P. Chaulet, and P. Nunn.** 1998. Global surveillance for antituberculosis-drug resistance, 1994–1997. N. Engl. J. Med. **338**:1641–1649.
24. **Parker, K. C., M. A. Bednarek, and J. E. Coligan.** 1994. Scheme for ranking potential HLA-A2 binding peptides based on independent binding of individual peptide side-chains. J. Immunol. **152**:163–175.
25. **Pascolo, S., N. Bervas, J. M. Ure, A. G. Smith, F. A. Lemonnier, and B. Pérarnau.** 1997. HLA-A2.1-restricted education and cytolytic activity of CD8$^+$ T lymphocytes from β2 microglobulin (β2m) HLA-A2.1 monochain transgenic H-2D^b β2m double knockout mice. J. Exp. Med. **185**:2043–2051.
26. **Ramalingam, B., K. R. Uma Devi, and A. Raja.** 2003. Isotype-specific anti-38 and 27 kDa (mpt51) response in pulmonary tuberculosis with human immunodeficiency virus coinfection. Scand. J. Infect. Dis. **35**:234–239.
27. **Rammensee, H. G., J. Bachmann, N. P. N. Emmerich, O. A. Bachor, and S. Stevanović.** 1999. SYFPEITHI: database for MHC ligands and peptide motifs. Immunogenetics **50**:213–219.
28. **Ruppert, J., J. Sidney, E. Celis, R. T. Kubo, H. M. Grey, and A. Sette.** 1993. Prominent role of secondary anchor residues in peptide binding to HLA-A2.1 molecules. Cell **74**:929–937.
29. **Salter, R. D., and P. Cresswell.** 1986. Impaired assembly and transport of HLA-A and -B antigens in a mutant T×B cell hybrid. EMBO. J. **5**:943–949.
30. **Smith, S. M., R. Brookes, M. R. Klein, A. S. Malin, P. T. Lukey, A. S. King, G. S. Ogg, A. V. S. Hill, and H. M. Dockrell.** 2000. Human CD8$^+$ CTL specific for the mycobacterial major secreted antigen 85A. J. Immunol. **165**:7088–7095.
31. **Smith, S. M., and H. M. Dockrell.** 2000. Role of CD8$^+$ T cells in mycobacterial infections. Immunol. Cell Biol. **78**:325–333.
32. **Sterne, J. A. C., L. C. Rodrigues, and I. N. Guedes.** 1998. Does the efficacy of BCG decline with time since vaccination? Int. J. Tuberc. Lung Dis. **2**:200–207.
33. **Stuber, G., S. Modrow, P. Höglund, L. Franksson, J. Elvin, H. Wolf, K. Kärre, and G. Klein.** 1992. Assessment of major histocompatibility complex class I interaction with Epstein-Barr virus and human immunodeficiency virus peptides by elevation of membrane H-2 and HLA in peptide loading-deficient cells. Eur. J. Immunol. **22**:2697–2703.
34. **Suzuki, M., T. Aoshi, T. Nagata, and Y. Koide.** 2004. Identification of murine H2-D^d- and H2-A^b-restricted T-cell epitopes on a novel protective antigen, MPT51, of *Mycobacterium tuberculosis*. Infect. Immun. **72**:3829–3837.
35. **Wiker, H. G., and M. Harboe.** 1992. The antigen 85 complex: a major secretion product of *Mycobacterium tuberculosis*. Microbiol. Rev. **56**:648–661.
36. **Wilson, R. A., W. N. Maughan, L. Kremer, G. S. Besra, and K. Fütterer.** 2004. The structure of *Mycobacterium tuberculosis* MPT51 (FbpC1) defines a new family of noncatalytic α/β hydrolases. J. Mol. Biol. **335**:519–530.
37. **World Health Organization.** 2007. WHO Report. 2007 Global tuberculosis control: surveillance, planning, financing. World Health Organization, Geneva, Switzerland. http://www.who.int/tb/publications/global_report/2007/pdf/full.pdf. Accessed 21 August 2007.

Editor: R. P. Morrison

Available online at www.sciencedirect.com
ScienceDirect
Cancer Letters 260 (2008) 137–145
CANCER Letters
www.elsevier.com/locate/canlet

Effective induction of anti-tumor immune responses with oligomannose-coated liposome targeting to intraperitoneal phagocytic cells

Yuzuru Ikehara [a,b,*], Nobumitsu Shiuchi [c], Sanae Kabata-Ikehara [a,b], Hayao Nakanishi [b], Naoaki Yokoyama [d], Hideaki Takagi [c], Toshi Nagata [e], Yukio Koide [e], Kiyotaka Kuzushima [f], Toshitada Takahashi [g], Kunio Tsujimura [e], Naoya Kojima [c]

[a] *Molecular Medicine Team of Research Center for Medical Glycoscience, National Institute of Advanced Industrial Science and Technology, Centeral 2-12, Room 211, 1-1-1 Umezono, Tsukuba, Japan*
[b] *Division of Oncological Pathology, Aichi Cancer Center Research Institute, Nagoya, Japan*
[c] *Department of Applied Biochemistry, The Institute of Glycotechnology, Tokai University, Hiratsuka, Japan*
[d] *Research Unit for Molecular Diagnosis, National Research Center for Protozoan Diseases, Obihiro University of Agriculture and Veterinary Medicine, Obihiro, Japan*
[e] *Department of Infectious Diseases, Hamamatsu University School of Medicine, Hamamatsu, Japan*
[f] *Division of Immunology, Aichi Cancer Center Research Institute, Nagoya, Japan*
[g] *Aichi Comprehensive Health Science Center of the Aichi Health Promotion Foundation, Aichi, Japan*

Received 2 July 2007; received in revised form 22 October 2007; accepted 29 October 2007

Abstract

We recently established a novel drug delivery system (DDS) using oligomannose-coated liposomes (OMLs) which are probably taken up by macrophages (Mϕ) to carry anti-cancer drugs to milky spots known as preferential metastatic sites of gastric cancers [Y. Ikehara, T. Niwa, L. Biao, S.K. Ikehara, N. Ohashi, T. Kobayashi, Y. Shimizu, N. Kojima, H. Nakanishi, A carbohydrate recognition-based drug delivery and controlled release system using intraperitoneal macrophages as a cellular vehicle, Cancer Res. 66 (2006) 8740–8748]. In the present study, we applied this intraperitoneal DDS for systemic cancer immunotherapy employing ovalbumin (OVA) as a model antigen. The cells taking up the OMLs containing FITC-OVA injected into the peritoneal cavity were predominantly Mϕ, as they showed adhesive characteristics and expressed F4/80 and CD11b almost exclusively. The phagocytic cells also took up bare OVA directly to the same extent as OML-enclosed OVA (OML-OVA), as it is a highly mannosilated protein. The phagocytic cells taking up OML-OVA, however, could activate OVA-specific $CD8^+$ (from OT-I: H-$2K^b$/$OVA_{257-264}$-specific) and $CD4^+$ (from OT-II: H-$2A^b$/$OVA_{323-339}$-specific) T cells much more effectively *in vitro* than those taking up bare OVA. Furthermore, only the mice pre-immunized with OML-OVA rejected E.G7-OVA (OVA-transfected EL4) but not EL4. These results indicate that

* Corresponding author. Address: Molecular Medicine Team of Research Center for Medical Glycoscience, National Institute of Advanced Industrial Science and Technology, Tsukuba, Japan. Tel.: +81 29 861 5853; Fax: +81 29 861 3462.
E-mail address: yuzuru-ikehara@aist.go.jp (Y. Ikehara).

0304-3835/$ - see front matter
doi:10.1016/j.canlet.2007.10.038

the OMLs can also be used as an effective antigen delivery system for cancer immunotherapy activating both CTL and Th subsets.

Keywords: Drug delivery system; Cancer vaccine; Immune responses to cancer; Oligomannose liposome

1. Introduction

While recent advances in tumor immunology enable us to identify tumor antigens recognized by T cells and understand the molecular and cellular bases of T cell-mediated anti-tumor responses, the clinical realization of effective immunotherapy for solid tumors has not yet been convincingly achieved [1,2]. Many $CD8^+$ and $CD4^+$ T cells recognizing tumor antigen in the context of MHC class I and II, respectively, have been reported, and the former are known to be a major effector of the adaptive anti-tumor immune responses [3–5]. $CD4^+$ T cells play an important role for the expansion and persistence of $CD8^+$ T cells, while some of them are known to function as regulatory cells [5–7]. Optimal anti-tumor immune responses are therefore considered to require the concomitant activation of both $CD8^+$ and $CD4^+$ T cells and the selective activation of $CD4^+$ T cells with helper but not regulatory functions [8]. Endogenous and exogenous antigens are presented as peptides preferentially by MHC class I and II, respectively, and most tumor antigen peptides are derived from the proteins expressed endogenously. Novel methods to make tumor antigens presented simultaneously by both MHC class I and II molecules are therefore needed for the concomitant activation of antigen-specific $CD8^+$ and $CD4^+$ T cells, and many attempts have been made for this purpose [2,3,8].

We recently developed a novel drug delivery system (DDS) using oligomannose-coated liposomes (OMLs) [9,10] which are effectively taken up by $F4/80^+$ intraperitoneal cells to carry anti-cancer drugs to milky spots known as a preferential metastatic site of gastric and ovarian cancers [9,11,12]. We demonstrated that this system could control the formation of overt metastasis of seeded gastric cancer cells at the extra-nodal lymphoid tissues such as the omentum [10].

In the present study, we applied this OML-based intraperitoneal DDS for cancer immunotherapy using ovalbumin (OVA) as a model antigen, aiming at the concomitant activation of antigen-specific $CD8^+$ and $CD4^+$ T cells. Peritoneal phagocytic cells took up OML containing OVA and then migrated into milky spots as previously reported. In addition, they activated both OVA-specific $CD8^+$ [13,14] and $CD4^+$ [15] T cells effectively *in vitro*. Spleen cells from OML-enclosed OVA (OML-OVA)-injected mice showed an effective killing activity against E.G7-OVA (OVA-transfected EL4) [16] but not EL4 [17] *in vitro*, and only the mice pre-immunized with OML-OVA rejected E.G7-OVA but not EL4 *in vivo*. In light of these results obtained *in vitro* and *in vivo*, the potential of our novel OML-based immunization method for the prevention of tumor metastasis is discussed.

2. Materials and methods

2.1. Mice

Female C57BL/6 (B6) mice ($H\text{-}2^b$) at 8–12 weeks of age were obtained from Charles River Japan Inc. (Yokohama, Japan) and kept under standard housing conditions. T cell receptor transgenic mice OT-I (specific for $H\text{-}2K^b/OVA_{257\text{-}264}$) [13,14] and OT-II ($H\text{-}2A^b/OVA_{323\text{-}339}$) [15] were obtained from the Jackson Laboratory (Bar Harbor, ME) and maintained under specific pathogen-free conditions. All animal experiments were performed under the experimental protocol approved by the Ethics Review Committee for Animal Experimentation of Aichi Cancer Center.

2.2. Cell lines

EL4 [17], a B6-derived thymoma cell line, was maintained in RPMI1640 medium (Invitrogen, Carlsbad, CA) supplemented with 8% fetal bovine serum, 0.2% L-glutamine, 100 U/ml penicillin, 100 μg/ml streptomycin, 0.1% Hepes, 0.1 mM non-essential amino acids, 1 mM sodium pyruvate, and 50 μM 2-ME (complete RPMI). EG.7-OVA (EL4 transfected with *OVA* gene) [16] was obtained from ATCC (Manassas, VA) and maintained in complete RPMI supplemented with 400 μg/ml G418 (Wako, Osaka, Japan) in a humidified 5% CO_2 incubator at 37 °C.

2.3. Man3-DPPE and liposome preparation

Dipalmitoylphosphatidylcholine (DPPC), cholesterol, and dipalmitoylphosphatidylethanolamine (DPPE) were purchased from Sigma–Aldrich (St. Louis, MO). Mannotriose (Man3: Manα1-6(Manα1-3)Man) was purchased from Funakoshi Co., Ltd. (Tokyo, Japan). Man3-DPPE was prepared by conjugation of the mannotriose with DPPE by reductive amination as described in previous papers [10,18]. The purity of Man3-DPPE was confirmed by high-performance thin-layer chromatography (Silica gel 60 HPTLC plate, MERCK, Darmstadt, Germany) and time-of-flight mass spectrometry (Auto FLEX, Bruker Daltonics, Bremen, Germany). The purified Man3-DPPE was quantified by determination of the phosphate contained.

Liposomes were prepared as described previously [10]. Briefly, a chloroform–methanol (2:1, v/v) solution containing 1.5 μmol of DPPC and 1.5 μmol of cholesterol was placed in a conical flask and dried by rotary evaporation. Subsequently, 2 ml ethanol containing 0.15 μmol of Man3-DPPE was added to the flask and evaporated to prepare a lipid film containing neoglycolipids. Procedures for protein-encasing of oligomannose-coated liposomes (OMLs) were performed as described previously [10]. The multilamellar vesicles were generated with either 200 μl of FITC-labelled or non-labelled OVA (5.0 mg/ml, Sigma–Aldrich), Alexa Fluor 680 (Molecular Probes, Eugene, OR)-labelled bovine serum albumin (BSA, 5 mg/ml, Sigma–Aldrich), or PBS in the dried lipid film by intense vortex dispersion. The multilamellar vesicles were extruded 10 times through polycarbonate membranes of 1 μm pore (Nucleopore, Pleasanton, CA). Liposomes entrapping proteins were separated from free untrapped proteins by four successive rounds of washing in PBS with centrifugation (20,000*g*, 30 min) at 4 °C. The amounts of entrapped proteins were measured using a modified Lowry protein assay reagent (Pierce, Rockford, IL) in the presence of 0.3% (w/v) sodium dodecyl sulfate using BSA as the standard.

2.4. Flow cytometry

One hour after intraperitoneal injection, peritoneal exudate cells (PEC) were recovered from B6 mice with 5 ml ice cold PBS. PEC were incubated on ice for 30 min with fluorescein-labelled antibodies against mouse hematopoietic cell lineage markers after blocking with mouse Fc Blocker (BD Biosciences, San Jose, CA) and then analysed on a FACS Calibur (BD Biosciences). The following monoclonal antibodies used in this study were purchased or kindly provided: anti-F4/80 (A3-1, Serotec Ltd., Oxford, UK), anti-MHC class II (M5/114.15.2, e-Bioscience, Boston, MA), anti-CD11b (M1/70.15, Caltag Laboratories, Burlingame, CA), anti-CD3ε (145-2C11, BD Biosciences), anti-CD19 (1D3, BD Biosciences), and anti-H-2K^{b}D^b (20-8-4S, Dr. E. Nakayama, Okayama University).

2.5. Macrophage depletion by plastic adhesion

PEC suspension (2×10^7 cells in 10 ml of complete RPMI) was poured into a 75 cm^2 tissue culture flask and incubated at 37 °C for 2 h in a humidified 5% CO_2 incubator. Non-adherent cells were collected with serum-free DMEM and subjected to FACS analysis.

2.6. In vitro activation of OVA-specific T cells

One hour after injection of either OML-encased OVA or bare OVA into the peritoneal cavity of B6 mice, PEC were recovered with 5 ml ice cold PBS. The PEC suspended in complete RPMI were seeded into a 96-well culture plate (5×10^5 cells in each well) and incubated at 37 °C for overnight in a humidified 5% CO_2 incubator. On the next day, non-adherent cells were washed out with complete RPMI, and co-cultured with 5×10^5 cells of either CD8$^+$ or CD4$^+$ T cells from the spleen of OT-I and OT-II mice, respectively. CD8$^+$ and CD4$^+$ T cells were prepared with the isolation kits for corresponding subsets (Miltenyi Biotec Inc., Auburn, CA). The supernatants were collected at 24, 48, and 72 h and assayed for IFN-γ production with Mouse IFN-γ ELISA kit (Pierce Biotechnology, Inc., Rockford, IL).

2.7. CTLs assay

B6 mice were immunized biweekly three times by intraperitoneal injection of 1 μg OVA in liposome/mouse with or without oligomannose coating. Spleen cells were isolated from the mice 1 week after the last challenge, and 1×10^6 spleen cells were stimulated with 10 μg OVA in 1 ml for 72 h. The effector cells thus prepared were co-cultured with target cells (E.G7-OVA or EL4) at various effector/target ratios for 8 h at 37 °C, and the cytotoxicity was measured with CytoTox96 Non-Radioactive Cytotoxicity assay kit (Promega, Madison, WI).

2.8. Tumor assay

Tumor cells (in 0.2 ml) were injected intradermally into the backs of mice with a 27 gauge needle. The diameter of the tumors was measured with Vernier calipers twice at right angles to calculate the mean diameter, and the survival time after tumor challenges was followed.

3. Results

3.1. OMLs are taken up preferentially by intraperitoneal macrophages

We showed that neoglycolipid-coated liposomes are ingested by intraperitoneal cells much more effectively than non-coated liposomes [10]. Of those, OMLs are incorporated most effectively, and the cells ingesting

OMLs are preferentially F4/80$^+$ and migrate into extranodal lymphoid tissues in the omentum after the uptake. We have also shown that the OML-ingesting cells are very useful drug delivery vehicles for cancer chemotherapy in the previous study [9,10]. To verify whether the OMLs are applicable also for cancer immunotherapy, we first analyzed in detail the peritoneal cells incorporating OMLs. Bovine serum albumin (BSA, Sigma–Aldrich) was labelled with Alexa Fluor 680, encased in OML and then injected into the peritoneal cavity of B6 mice. One hour after the injection of OMLs containing Alexa Fluor 680-labelled BSA, PEC were collected and analyzed. As shown in Fig. 1A, PEC were divided into three groups based on the incorporation of OMLs. When adherent cells were removed by plastic dish adherence, only the population with higher OML uptake (R1) disappeared (Fig. 1B). In addition, most cells of R1 express F4/80 and CD11b but not CD3 and CD19 (Fig. 1C), suggesting that R1 population preferentially consists of macrophages (Mϕ). The PEC with lower OML uptake (R2) did not express F4/80, and nearly 2/3 of them were considered to be B cells because of their CD19 expression. These results together confirmed that OMLs injected into the peritoneal cavity were ingested preferentially by Mϕ, and also indicate that OML is a good vehicle for the phagocytosis of non-glycosylated proteins.

3.2. *Phagocytic cells ingesting OMLs activate both CD8 and CD4 T cells in vitro in an antigen-specific manner*

We next analyzed the antigen-presenting capacity of the phagocytic cells ingesting OMLs containing ovalbumin (OVA) as an antigen. CD8$^+$ T cells from OT-I (a transgenic strain of T cell receptor (TCR) recognizing $OVA_{257-264}$ peptide presented by H-2K^b) and CD4$^+$ T cells from OT-II (a transgenic strain of TCR recognizing $OVA_{323-339}$ peptide presented by H-2A^b) were used as responder cells. When these T cells were co-cultured with adherent cells enriched from PEC of the mouse intraperitoneally injected with OML-encased OVA (OML-OVA), both CD8$^+$ and CD4$^+$ T cells produced large amounts of IFN-γ (Fig. 2). Though adherent cells from the mice injected with soluble OVA also stimulated both CD8$^+$ and CD4$^+$ T cells, much higher amounts of OVA were needed compared to those from the mice injected with OML-OVA. Mϕ ingesting OML-OVA are supposed to

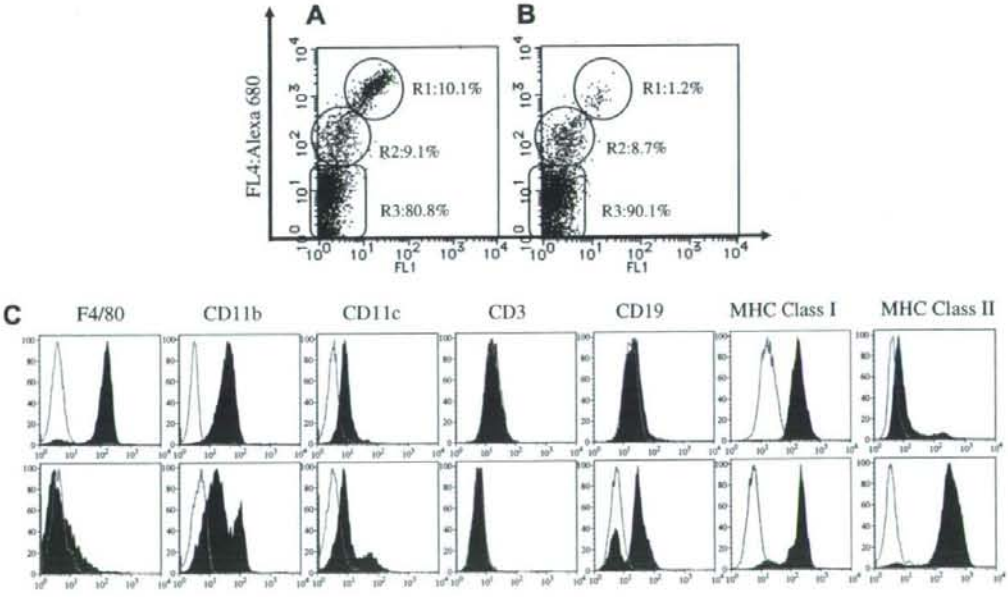

Fig. 1. OMLs injected into the peritoneal cavity were ingested preferentially by adhesive cells. One hour after injection of OMLs containing Alexa Fluor 680-labelled BSA, PEC were collected and their fluorescence was analyzed by flow cytometry (A). Non-adherent PEC were further isolated by plastic adherence for 2 h and analyzed (B). (C) Phenotypic analysis of PEC derived from OML-injected mice. One hour after injection of OMLs containing Alexa Fluor 680-labelled OVA, PEC were collected and stained with mAbs indicated. As shown in (A) and (B), PEC were divided into three groups based on their fluorescence intensity of Alexa Fluor 680, and the surface phenotypes of R1 and R2 were further analyzed.

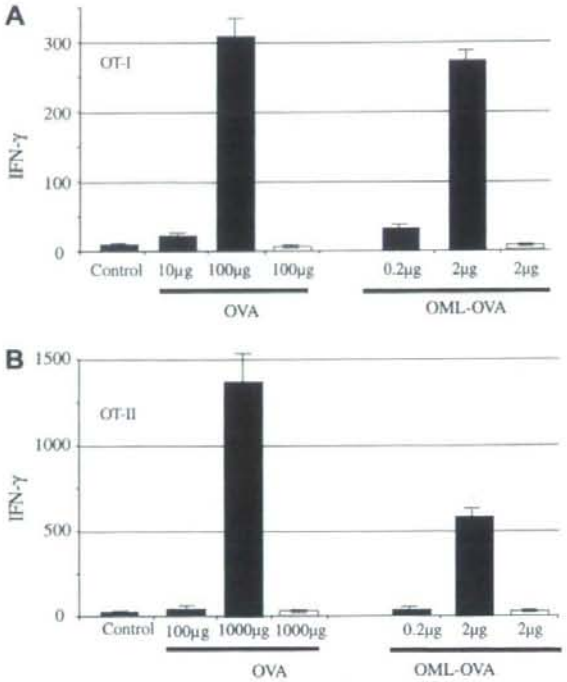

Fig. 2. Mϕ ingesting OVA encased in OML activate OVA-specific $CD8^+$ and $CD4^+$ T cells much more effectively than those ingesting soluble OVA. One hour after intraperitoneal injection of antigens, PEC were prepared from mice, and adherent cells were enriched by plastic adherence. $CD8^+$ and $CD4^+$ T cells were purified from spleen of OT-I (A) and OT-II (B), respectively, co-cultured (closed bar) with adherent PEC or cultured adherent PEC alone (open bar) for 24 h, and then production of IFN-γ in supernatants was tested by ELISA. PEC recovered from mice without any treatment was used as control. OML-OVA, OVA encased in OML; OVA, OVA; control, OML containing PBS. The graph shows the average and standard error from three independent experiments.

present antigen effectively also *in vivo*, as they effectively induced proliferation responses of OVA-specific $CD8^+$ T cells in the spleens of OT-I mice (Supplement Figure 1).

We next analyzed the uptake efficiency of OML-encased and soluble OVA and found that peritoneal phagocytic cells effectively uptake OVA irrespective of sugar encapsulation (Fig. 3). The uptake of soluble OVA is probably mediated by mannose receptors, as it is known as a highly mannosylated protein [19]. These results together indicate that OML-mediated ingestion promotes the presentation of OVA peptides by both MHC class I and II molecules by enhancing the antigen processing but not the uptake efficiency.

3.3. Induction of antigen-specific cytotoxic T lymphocytes (CTL) in vitro by OML-mediated immunization

We next performed CTL assay to detect OVA-specific T cells in the spleen. Only the spleen cells from mice immunized with OML-OVA but not bare liposome (BL)-encased OVA showed cytotoxicity against E.G7-OVA. The spleen cells from neither group showed cytotoxicity against EL4, confirming that OVA-specific CTL can be effectively induced *in vivo* by OML-OVA immunization (Fig. 4).

3.4. OML-mediated immunization induces antigen-specific anti-tumor immunity in vivo

We finally examined whether intraperitoneal immunization with OMLs also induces antigen-specific anti-tumor immunity *in vivo*. Mice were immunized intraperitoneally with OVA with or without OML encasing and then challenged with E.G7-OVA or EL4. As shown in Fig. 5, only the mice immunized with OML-OVA survived for more than 70 days when challenged with E.G7-OVA, while naïve and bare OVA-immunized mice died within 55 days. All the mice including those immunized with OML-OVA died within 30 days when challenged with EL4, indicating that the rejection of

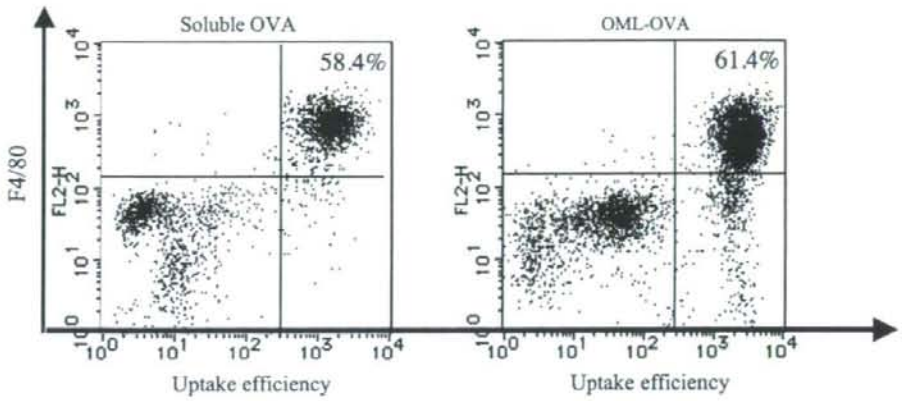

Fig. 3. Peritoneal F4/80$^+$ cells uptake OVA effectively irrespective of carbohydrate encapsulation. One hour after injection of either soluble FITC-OVA (20 μg) or OML-encapsulated FITC-OVA (20 μg) into the peritoneal cavity of B6 mice, uptake efficiency of FITC-OVA by peritoneal cells was analyzed by flow cytometry together with F4/80 expression.

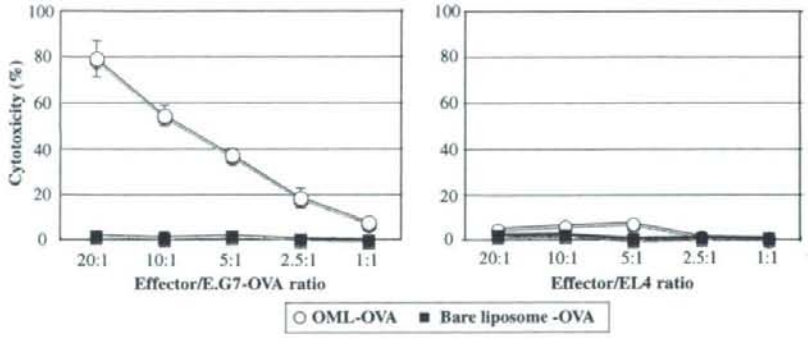

Fig. 4. OML-OVA-generated OVA-specific cytotoxicity. B6 mice were immunized biweekly three times by intraperitoneal injection of 1 μg OVA encased in oligomannose-coated (OML-OVA, open symbols) or bare liposomes (bare liposome-OVA, closed symbols). Spleen cells were isolated from mice one week after the last challenge, and 1×10^6 cells were stimulated with 10 μg OVA in 1 ml for 72 h. The graph shows the average and standard error from three independent experiments.

E.G7-OVA is OVA-specific. These results together showed that OML-mediated immunization can induce systemic immune response robust enough to protect mice from tumor challenge in an antigen-specific manner.

4. Discussion

In this study, we demonstrated that our novel OML-based drug delivery system (DDS) targeted to intraperitoneal phagocytic cells can also be used for the induction of systemic immune responses. After ingesting OML-encased OVA (OML-OVA), intraperitoneal phagocytic cells to extra-nodal lymphoid tissues in abdominal cavity and presented OVA-derived peptides in the context of both MHC class I and II molecules. Only the mice pre-immunized with OML-OVA rejected E.G7-OVA but not EL4 challenged subcutaneously. These results together indicate that the OMLs can be used as an effective antigen delivery system for immunotherapy activating both CTL and Th subsets. Fig. 6 shows the plausible induction process of anti-tumor immunity starting from phagocytic cells triggered by OML injection.

OMLs are very useful not only for the promotion of non-glycosylated protein uptake by antigen-presenting cells but also for the enhancement of antigen-processing of encased antigens. Endogenous

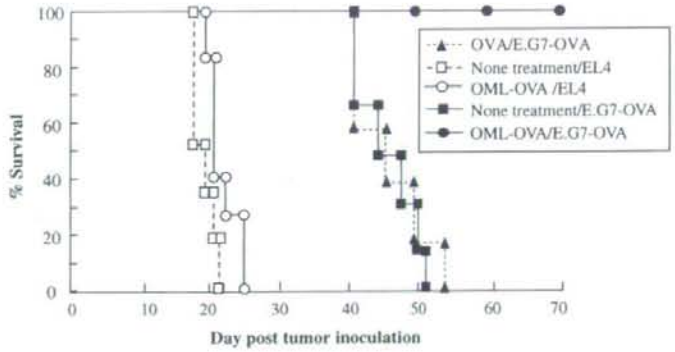

Fig. 5. OML-mediated immunization induces antigen-specific anti-tumor immunity *in vivo*. OML-OVA-immunized (circles) and naïve (squares) mice were challenged with E.G7-OVA (closed circles and squares) or EL4 cells (open circles and squares). As a control, mice were immunized with soluble OVA and challenged with E.G7-OVA (closed triangles).

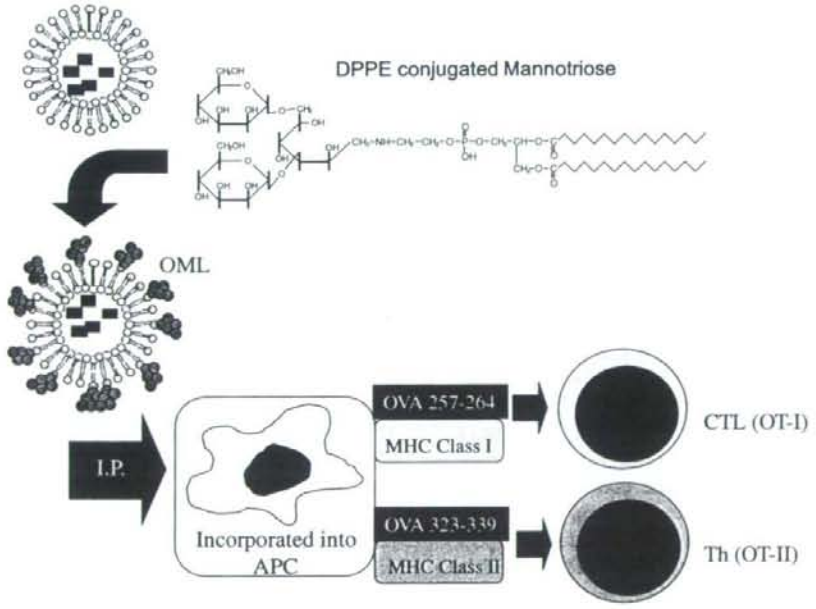

Fig. 6. Possible mechanism of OML-based vaccine delivery. Coating of bare liposomes with DPPE-conjugated mannotriose facilitates functions of intraperitoneal macrophages, resulting in antigen-specific activation of both CTL and Th populations.

and exogenous antigens are presented preferentially by MHC class I and II, respectively. OML-OVA, however, were effectively directed to both pathways, even when added exogenously. This advantage of OML-mediated immunization will hopefully facilitate the simultaneous activation of tumor antigen-specific $CD4^+$ and $CD8^+$ T cells as shown here with OVA. It is also very interesting to study the mechanism by which OML-mediated ingestion of antigens enhances the antigen presentation by both MHC molecules [20–22]. So far, we observed the up-regulation of CD80 and CD86 on OML-ingesting cells (in press on Cytokine, H. Takagi et al.), but it seems very important to know the additional signals to

make antigen presenting cells more immunogenic [23]. Additional adjuvant effects of various cytokines and/or toll-like receptor ligands on OML-mediated immunization are now being investigated.

Another advantage of OML-mediated immunization is Th1-skewing of the cytokine profiles. Indeed, OT-I and OT-II T cells stimulated with antigen-presenting cells ingesting OML-OVA produced IFN-γ but not IL-4 or IL-10 (unpublished observation). Moreover, our previous study demonstrated that the OML-mediated immunization protects BALB/c mice against *Leishmania major* infection, possibly due to the Th1-skewing of immune responses [24]. We observed that phagocytic cells ingesting OML preferentially produce IL-12 (unpublished observation), suggesting this cytokine is a key of Th1-skewing as reported previously [25]. Further investigation of the mechanism of this Th1-skewing of immune responses induced by OML-mediated immunization is currently underway.

Cells belonging to the monocyte-Mϕ lineage have been known to be heterogeneous, reflecting the plasticity and versatility of these cells in response to various microenvironmental signals [26]. Mϕ are now roughly categorized into M1 and M2 based on their functional properties, and several studies revealed that M1 and M2 promote type I and type II Th responses, respectively [27–29]. It is also reported that M1 and M2 are prone to induce inflammatory and immunoregulatory responses, respectively [29]. A possible concern of our DDS system is therefore the protumoral effects by M2 with antigen-encased OMLs, as they are supposed to express macrophage mannose receptors induced by IL-4 [30]. Although at least our *in vitro* study clearly showed OML-mediated skewing to type I immune responses, more precise investigation including the conditions for M1 polarization should be done especially in tumor-bearing mice. In addition, characteristics of the small population of non-Mϕ cells ingesting OMLs should be investigated as well.

In order to use our DDS in clinical study, the best administration routes should be determined to pursue repetitive vaccination while avoiding possible side effects. As generally acknowledged, intraperitoneal administration is accompanied with a high risk of side effects such as catheter-related complications, and abdominal pain [31]. In this connection, we have already obtained anti-tumor effects by subcutaneous injection of OML-OVA similar to those by intraperitoneal injection. However, side effects induced by subcutaneous injection of OMLs should be further investigated to assure their safe clinical application.

In the previous study, we reported that the formation of intraperitoneal metastasis of seeded gastric cancer cells in milky spots can be controlled with OMLs containing anti-cancer drugs [10]. In the present study, we have further extended the possibility of OMLs for the immunotherapy of systemic metastasis and existing tumor cells aside from milky spots. Oligomannose coating of liposomes showed the best uptake efficiency by intraperitoneal Mϕ among the neoglycolipids so far tested, and the encased antigen was effectively presented by both MHC class I and II molecules. However, the additional effects for immune responses by other neoglicolipids (shown here) have not been studied at all so far. We have a great interest in their effects on immune responses and are seeking sugar materials with immunoregulatory properties. If such materials are found, we believe that further study of our sugar-coated liposome technology will find it also to be applicable for antigen-specific regulation of autoimmune diseases and allergy.

Acknowledgments

We thank Ms. Y. Matsudaira and Ms. K. Nishida for their excellent technical assistance. This work was supported by the Industrial Technology Research Grant Program in 04' from the New Energy and Industrial Technology Development Organization (NEDO) of Japan, and in part by a grant for Hi-tech research program from Tokai University and by the Program for Promotion of Basic Research Activities for Innovative Biosciences (PROBRAIN). The costs of publication of this article were defrayed in part by the payment of page charges. This article must therefore be hereby marked advertisement in accordance with 18 U.S.C. Section 1734 solely to indicate this fact.

Appendix A. Supplementary data

Supplementary data associated with this article can be found, in the online version, at doi:10.1016/j.canlet.2007.10.038.

References

[1] L. Gattinoni, D.J. Powell Jr., S.A. Rosenberg, N.P. Restifo, Adoptive immunotherapy for cancer: building on success, Nat. Rev. Immunol. 6 (2006) 383–393.

[2] S.A. Rosenberg, J.C. Yang, N.P. Restifo, Cancer immunotherapy: moving beyond current vaccines, Nat. Med. 10 (2004) 909–915.
[3] S.A. Rosenberg, Progress in the development of immunotherapy for the treatment of patients with cancer, J. Intern. Med. 250 (2001) 462–475.
[4] T. Boon, P.G. Coulie, B.J. Van den Eynde, P. van der Bruggen, Human T cell responses against melanoma, Annu. Rev. Immunol. 24 (2006) 175–208.
[5] D.M. Pardoll, S.L. Topalian, The role of CD4+ T cell responses in antitumor immunity, Curr. Opin. Immunol. 10 (1998) 588–594.
[6] R.F. Wang, G. Peng, H.Y. Wang, Regulatory T cells and toll-like receptors in tumor immunity, Semin. Immunol. 18 (2006) 136–142.
[7] S. Sakaguchi, R. Setoguchi, H. Yagi, T. Nomura, Naturally arising Foxp3-expressing CD25+CD4+ regulatory T cells in self-tolerance and autoimmune disease, Curr. Top. Microbiol. Immunol. 305 (2006) 51–66.
[8] A.M. Leen, C.M. Rooney, A.E. Foster, Improving T cell therapy for cancer, Annu. Rev. Immunol. 25 (2007) 243–265.
[9] Y. Ikehara, N. Kojima, Development of a novel oligomannose-coated liposome-based anticancer drug-delivery system for intraperitoneal cancer, Curr. Opin. Mol. Ther. 9 (2007) 53–61.
[10] Y. Ikehara, T. Niwa, L. Biao, S.K. Ikehara, N. Ohashi, T. Kobayashi, Y. Shimizu, N. Kojima, H. Nakanishi, A carbohydrate recognition-based drug delivery and controlled release system using intraperitoneal macrophages as a cellular vehicle, Cancer Res. 66 (2006) 8740–8748.
[11] L.F. Krist, M. Kerremans, D.M. Broekhuis-Fluitsma, I.L. Eestermans, S. Meyer, R.H. Beelen, Milky spots in the greater omentum are predominant sites of local tumour cell proliferation and accumulation in the peritoneal cavity, Cancer Immunol. Immunother. 47 (1998) 205–212.
[12] A. Hagiwara, T. Takahashi, K. Sawai, H. Taniguchi, M. Shimotsuma, S. Okano, C. Sakakura, H. Tsujimoto, K. Osaki, S. Sasaki, et al., Milky spots as the implantation site for malignant cells in peritoneal dissemination in mice, Cancer Res. 53 (1993) 687–692.
[13] K.A. Hogquist, S.C. Jameson, W.R. Heath, J.L. Howard, M.J. Bevan, F.R. Carbone, T cell receptor antagonist peptides induce positive selection, Cell 76 (1994) 17–27.
[14] S.R. Clarke, M. Barnden, C. Kurts, F.R. Carbone, J.F. Miller, W.R. Heath, Characterization of the ovalbumin-specific TCR transgenic line OT-I: MHC elements for positive and negative selection, Immunol. Cell Biol. 78 (2000) 110–117.
[15] M.J. Barnden, J. Allison, W.R. Heath, F.R. Carbone, Defective TCR expression in transgenic mice constructed using cDNA-based alpha- and beta-chain genes under the control of heterologous regulatory elements, Immunol. Cell Biol. 76 (1998) 34–40.
[16] M.W. Moore, F.R. Carbone, M.J. Bevan, Introduction of soluble protein into the class I pathway of antigen processing and presentation, Cell 54 (1988) 777–785.
[17] P.A. Gorer, Studies in antibody response of mice to tumour inoculation, Br. J. Cancer 4 (1950) 372–379.
[18] T. Mizuochi, R.W. Loveless, A.M. Lawson, W. Chai, P.J. Lachmann, R.A. Childs, S. Thiel, T. Feizi, A library of oligosaccharide probes (neoglycolipids) from *N*-glycosylated proteins reveals that conglutinin binds to certain complex-type as well as high mannose-type oligosaccharide chains, J. Biol. Chem. 264 (1989) 13834–13839.
[19] T. Tai, K. Yamashita, M. Ogata-Arakawa, N. Koide, T. Muramatsu, S. Iwashita, Y. Inoue, A. Kobata, Structural studies of two ovalbumin glycopeptides in relation to the endo-beta-*N*-acetylglucosaminidase specificity, J. Biol. Chem. 250 (1975) 8569–8575.
[20] M.C. Tan, A.M. Mommaas, J.W. Drijfhout, R. Jordens, J.J. Onderwater, D. Verwoerd, A.A. Mulder, A.N. van der Heiden, T.H. Ottenhoff, M. Cella, A. Tulp, J.J. Neefjes, F. Koning, Mannose receptor mediated uptake of antigens strongly enhances HLA-class II restricted antigen presentation by cultured dendritic cells, Adv. Exp. Med. Biol. 417 (1997) 171–174.
[21] A. Lanzavecchia, Mechanisms of antigen uptake for presentation, Curr. Opin. Immunol. 8 (1996) 348–354.
[22] F. Sallusto, M. Cella, C. Danieli, A. Lanzavecchia, Dendritic cells use macropinocytosis and the mannose receptor to concentrate macromolecules in the major histocompatibility complex class II compartment: downregulation by cytokines and bacterial products, J. Exp. Med. 182 (1995) 389–400.
[23] J.S. Lam, M.K. Mansour, C.A. Specht, S.M. Levitz, A model vaccine exploiting fungal mannosylation to increase antigen immunogenicity, J. Immunol. 175 (2005) 7496–7503.
[24] Y. Shimizu, K. Yamakami, T. Gomi, M. Nakata, H. Asanuma, T. Tadakuma, N. Kojima, Protection against *Leishmania major* infection by oligomannose-coated liposomes, Bioorg. Med. Chem. 11 (2003) 1191–1195.
[25] G. Trinchieri, Interleukin-12 and the regulation of innate resistance and adaptive immunity, Nat. Rev. Immunol. 3 (2003) 133–146.
[26] F.O. Martinez, S. Gordon, M. Locati, A. Mantovani, Transcriptional profiling of the human monocyte-to-macrophage differentiation and polarization: new molecules and patterns of gene expression, J. Immunol. 177 (2006) 7303–7311.
[27] S. Gordon, Alternative activation of macrophages, Nat. Rev. Immunol. 3 (2003) 23–35.
[28] A. Mantovani, A. Sica, M. Locati, Macrophage polarization comes of age, Immunity 23 (2005) 344–346.
[29] A. Mantovani, A. Sica, S. Sozzani, P. Allavena, A. Vecchi, M. Locati, The chemokine system in diverse forms of macrophage activation and polarization, Trends Immunol. 25 (2004) 677–686.
[30] M. Stein, S. Keshav, N. Harris, S. Gordon, Interleukin 4 potently enhances murine macrophage mannose receptor activity: a marker of alternative immunologic macrophage activation, J. Exp. Med. 176 (1992) 287–292.
[31] S.A. Cannistra, Intraperitoneal chemotherapy comes of age, N. Engl. J. Med. 354 (2006) 77–79.

Microbial Pathogenesis 46 (2009) 6–12

Contents lists available at ScienceDirect

Microbial Pathogenesis

journal homepage: www.elsevier.com/locate/micpath

Virulence of *Mycobacterium avium* complex strains isolated from immunocompetent patients

Yoshitaka Tateishi [a,b,*], Yukio Hirayama [a], Yuriko Ozeki [a,c], Yukiko Nishiuchi [a,d], Mamiko Yoshimura [a], Jing Kang [a], Atsushi Shibata [a], Kazuto Hirata [e], Seigo Kitada [b], Ryoji Maekura [b], Hisashi Ogura [f], Kazuo Kobayashi [g], Sohkichi Matsumoto [a,*]

[a] Department of Bacteriology, Osaka City University Graduate School of Medicine, 1-4-3 Asahi-machi, Abeno-ku, Osaka 545-8585, Japan
[b] Department of Internal Medicine, National Hospital Organization Toneyama National Hospital, 5-1-1 Toneyama, Toyonaka, Osaka 560-8552, Japan
[c] Sonoda Women's University, 7-29-1 Minamitsukaguchi-cho, Amagasaki, Hyogo 661-8520, Japan
[d] Toneyama Institute for Tuberculosis Research, Osaka City University Medical School, Toyonaka 5-1-1, Toneyama, Toyonaka, Osaka 560-8552, Japan
[e] Department of Respiratory Medicine, Osaka City University Graduate School of Medicine, 1-4-3 Asahi-machi, Abeno-ku, Osaka 545-8585, Japan
[f] Department of Virology, Osaka City University Graduate School of Medicine, 1-4-3 Asahi-machi, Abeno-ku, Osaka 545-8585, Japan
[g] Department of Immunology, National Institute of Infectious Diseases, 1-23-1, Toyama, Shinjuku-ku, Tokyo 162-8640, Japan

ARTICLE INFO

Article history:
Received 6 August 2008
Received in revised form
29 September 2008
Accepted 2 October 2008
Available online 1 November 2008

Keywords:
Mycobacterium avium complex
Virulence
Clinical isolates
Immunocompetent humans
Pulmonary disease

ABSTRACT

Mycobacterium avium complex (MAC) disease has been increasing worldwide not only in immunocompromised but also in immunocompetent humans. However, the relationship between mycobacterial strain virulence and disease progression in immunocompetent humans is unclear. In this study, we isolated 6 strains from patients with pulmonary MAC disease. To explore the virulence, we examined the growth in human THP-1 macrophages and pathogenicity in C57BL/6 mice. We found that one strain, designated 198, which was isolated from a patient showing the most progressive disease, persisted in THP-1 cells. In addition, strain 198 grew to a high bacterial load with strong inflammation in mouse lungs and spleens 16 weeks after infection. To our knowledge, strain 198 is the first isolated MAC strain that exhibits hypervirulence consistently for the human patient, human macrophages *in vitro*, and even for immunocompetent mice. Other strains showed limited survival and weak virulence both in macrophages and in mice, uncorrelated to disease progression in human patients. We demonstrated that there is a hypervirulent clinical MAC strain whose experimental virulence corresponds to the serious disease progression in the patients. The existence of such strain suggests the involvement of bacterial virulence in the pathogenesis of pulmonary MAC disease in immunocompetent status.

1. Introduction

Mycobacterium avium complex (MAC) is the most common cause of human infection due to nontuberculous mycobacteria. Initially MAC was regarded as only an opportunistic pathogen, primarily in acquired immunodeficiency syndrome (AIDS) patients [1]; however, it has now been shown to cause progressive pulmonary disease even in immunocompetent humans [2]. The American Thoracic Society indicates a wide range of clinical manifestation in patients with non-AIDS MAC disease; some patients keep a stable condition for years, whereas others progress their illness rapidly [3]. Furthermore, MAC infection can be more difficult to treat than *M. tuberculosis* due to even fewer available anti-microbial agents [3].

The pathogenesis of MAC infection has been recently investigated with respect to the host immune response. Interferon-gamma (IFN-γ) activates macrophages to produce proteolytic enzymes and other metabolites, which exhibit mycobactericidal effects. Tumor necrosis factor-alpha (TNF-α), of which production is also stimulated by IFN-γ, augments the bactericidal capacity of macrophages and plays a key role in the induction of the acquired immune response against mycobacteria [4]. A defective IFN-γ response has been shown recently to cause disseminated MAC disease in IFN-γ knock out mice and in humans with genetic mutations of IFN-γ receptor [5,6] or autoantibodies to IFN-γ in some young non-AIDS patients [7,8]. In addition to that, the activity of interleukin-10 (IL-10), which is known to inhibit cytokine synthesis by IFN-γ-producing type1 helper T cells (Th1 cells), has been shown to increase susceptibility to MAC infection in immunocompetent mice [9].

* Corresponding authors. Department of Bacteriology, Osaka City University, Graduate School of Medicine, 1-4-3 Asahi-machi, Abeno-ku, Osaka 545-8585, Japan. Tel.: +81 6 6645 3746; fax: +81 6 6645 3747.
E-mail address: y-tateishi@med.osaka-cu.ac.jp (Y. Tateishi).

0882-4010/$ – see front matter © 2008 Elsevier Ltd. All rights reserved.
doi:10.1016/j.micpath.2008.10.007

Besides genetic factors of the host, bacterial virulence should play an important role for the development of MAC disease. While isolates of *M. tuberculosis* are genetically homogeneous at the nucleotide level [10], MAC has high genetic diversity, including the presence of multiple plasmids [11], and thus likely to have a large corresponding diversity in virulence. In the most complete study examining virulence, forty-one MAC isolates from the environment as well as infected humans and animals were compared for virulence in C57BL/6 mice by intravenous injection [12]. Monitoring of the virulence by CFU counts in lungs, livers, and spleens over 4 months revealed three virulence phenotypes; high (logarithmically increasing load), intermediate (chronic infection at a constant load), and low (initial load increase followed by a decrease until clearance). In addition, clinical studies have suggested severe disease outcome in patients infected with some specific strain type of MAC. For example, MAC serovars 1, 4, and 8 *Mycobacterium avium* are associated with disease severity in AIDS patients [13], and a serovar 4 *M. avium* isolate from an AIDS patient was more invasive and proliferative in blood mononuclear cell-derived human macrophages than a serovar 2 strain from chickens [14]. In non-AIDS MAC disease, *Mycobacterium intracellulare* is associated with greater disease progression [15], and moreover, our previous prospective study on 68 non-AIDS patients suggests that serovar 4 *M. avium* is linked to greater disease progression with a pulmonary MAC infection [16]. Taking these previous data into consideration, we hypothesize that relatively hypervirulent MAC strains exist and may be associated with serious disease progression in immunocompetent patients. In order to elucidate the involvement of mycobacterial virulence in the pathogenesis of human pulmonary MAC disease, in this study we examined the difference of mycobacterial virulence of clinical isolates from patients with different disease types using human macrophages and immunocompetent mice.

2. Results

2.1. Characteristics of mycobacterial strains

Six clinical isolates of MAC were isolated from sputum of non-AIDS patients with pulmonary MAC disease, and designated 27, 33, 36, 198, 288, and 347 (Table 1). Strains 33, 198 and 288 were derived from patients with progressive disease against combination chemotherapy recommended by the American Thoracic Society guideline (progressive type) [3]. The patients with progressive disease exhibited higher levels of erythrocyte sedimentation rate (ESR), diffuse and severe pulmonary lesions in chest X-ray findings, and numerous bacteria in the sputum. The patient infected with strain 198 exhibited the most serious disease outcome among study patients in that a right pneumonectomy was needed to prevent disease progression. Strains 27, 36, and 347 were derived from patients with little progression of disease without chemotherapy (silent type). They exhibited lower levels of ESR, segmental pulmonary lesions in chest X-ray findings, and fewer bacteria in the sputum. The isolates belonging to the progressive type consisted of *M. intracellulare* unclassified serovar similar to serovar 12 (strain 198) and *M. avium* apolar type (strains 33 and 288). The isolates belonging to the silent type consisted of *M. intracellulare* serovar 1 (strain 27) and *M. avium* apolar type (strains 36 and 347). For comparison, we employed 2 veterinary strains of *M. avium* ATCC 25291 (serovar 2) as a highly virulent strain in mice [12] and ATCC 35767 (serovar 4) as a low virulent strain. Four clinical isolates other than strains 33 and 347, and ATCC 25291 formed the transparent colony morphology. Strain 33 produced both transparent and rough colony morphologies. Strain 347 and ATCC 35767 displayed smooth opaque colony morphology.

2.2. Growth of clinical isolates in 7H9 broth

All strains showed logarithmic growth from 3 days after culture in 7H9 broth (Table 2). At day 5, two isolates from progressive type (strains 198 and 288) and one isolate from silent type (strain 36) grew significantly slower than ATCC 25291 ($P < 0.005$), and all clinical strains grew significantly slower than ATCC 35767 ($P < 0.0001$). The growth of strain 198 at day 5 was significantly slower than that of strain 27 ($P = 0.001$), and was not significantly different from that of other clinical isolates.

2.3. Virulence of clinical isolates in THP-1 monocyte-derived macrophages

We next studied intracellular survival of the isolates. THP-1 cells, a human monocytic cell line, were differentiated into macrophages by treatment with phorbol 12-myristate 13-acetate (PMA) and infected with MAC strains. Strain 198 grew in THP-1 cells significantly higher than any other strains during 7 days of infection ($P < 0.0001$) (Table 3). Strain 198 grew to approximately 20-fold during 2 days of infection ($P = 0.005$), and even at day 7, it kept the same level of bacterial load as day 0. Strain 36 also grew to approximately 2-fold during 2 days of infection ($P = 0.008$); however, it was rapidly eliminated at day 7, similar to the other strains except for strain 198. There was no significant difference in

Table 1
Characteristics of isolated strains and clinical findings.

Isolates	Species and serovar	Age	Sex	Duration of illness (years)	Erythrocyte sedimentation rate (mm/h)	Chest X-ray findings[a]	Sputum[b]	
							Smear	Culture
Progressive type								
33	*M. avium* apolar type	58	M	17	62	Advanced	2+	3+
198	*M. intracellulare* unclassified serovar[c]	62	F	3	108	Advanced	2+	2+
288	*M. avium* apolar type	56	F	12	78	Advanced	2+	2+
Silent type								
27	*M. intracellulare* serovar 1	67	F	17	50	Moderate	-	1+
36	*M. avium* apolar type	54	F	9	29	Moderate	-	1+
347	*M. avium* apolar type	79	F	14	50	Moderate	1+	1+

Data and sputum samples were collected at the enrollment of the study in 2003.

[a] Advanced chest X-ray findings were defined as bilateral cavities, giant cavities, or bilateral bronchiectasis, and moderate findings were defined as focal inflammation, small or fewer cavities, or mild bronchiectasis.

[b] Smear findings of sputum were defined as follows in high performance fields of microscopy; -: no bacteria in all fields, 1+: less than one bacteria in several fields, 2+: approximately 1–12 bacteria in one field. Culture findings were defined as follows using Ogawa egg agar; 1+: colonies less than 200, 2+: colonies more than 200 and less than 500, 3+: colonies more than 500 and less than 2000.

[c] The serovar of strain 198 was identified as a new type similar to serovar 12 determined by the liquid chromatography/mass spectrometry.

Table 2
Growth rate of MAC in 7H9 broth.

Strain	Ratio of CFUs at[a]		
	Day 1	Day 3	Day 5
33	0.91 ± 0.28	38 ± 0.86	63 ± 10
198	0.93 ± 0.17	12 ± 1.9	18 ± 4.0
288	0.85 ± 0.20	4.3 ± 1.9	16 ± 0.95
27	1.1 ± 0.25	7.3 ± 2.2	120 ± 21
36	0.83 ± 0.093	5.4 ± 0.21	11.0 ± 1.7
347	0.96 ± 0.16	2.7 ± 1.1	44 ± 19
25291	1.6 ± 0.25	4.8 ± 0.24	110 ± 16*
35767	0.97 ± 0.12	11 ± 3.0	370 ± 43**

* Significantly different ($P < 0.005$) from values for strain 198, 288, and 36 as calculated by Scheffé's test.
** Significantly different ($P < 0.0001$) from values for all clinical strains as calculated by Scheffé's test.
[a] Means ± standard deviations of the ratio of CFUs to those at day 0.

the growth rate among these strains except strain 198 during infection.

On light microscopic observation, THP-1 cell morphologies were not different between infected and uninfected cells (data not shown). We then assessed cytotoxicity by the levels of lactate dehydrogenase (LDH) released into the culture supernatants at day 7. The LDH release was detectable in strain 33 and the laboratory strains (strain 33; 5.8 ± 1.5%, ATCC 25291; 11 ± 1.0%, ATCC 35767; 12 ± 1.9%, without significant difference among these strains); however, it was not detectable in other clinical isolates.

2.4. Pathogenesis of clinical isolates in mice

Female C57BL/6 mice were infected by intratracheal instillation with each strain. Bacterial load in lungs, livers, and spleens were evaluated, and histological inflammation was visually analyzed in 5-mice per strain at defined time points during 16 weeks of infection. There was no significant difference in lung CFUs among strains tested 1 day after the inoculation.

Strain 198 showed high bacterial load, and tended to increase gradually both in lungs and spleens during 16 weeks of infection ($P = 0.08$ between day 1 and 16 weeks) (Fig. 1). Strain 198 was loaded in lungs significantly higher than strain 27 ($P = 0.04$) and 33 ($P = 0.0006$) at 8 weeks of infection, and than strain 33 ($P = 0.0009$), 288 ($P = 0.001$), 36 ($P = 0.0003$), and 347 ($P = 0.004$) at 16 weeks. Histologically, strain 198 induced strong inflammation in lungs, which was paralleled with bacterial loads (Fig. 2). ATCC 25291, known as highly a virulent strain in mice [12], showed initial reduction of bacterial load in lungs at 4 weeks of infection ($P = 0.01$ between day 1 and 4 weeks) and rapid increase in bacterial load in lungs after 4 weeks of infection. ATCC 25291 was comparatively virulent to strain 198 with respect to the high bacterial load in lungs and spleens, and severe pulmonary inflammation at 16 weeks of infection. By contrast, other clinical isolates did not increase profoundly in lung CFUs; however, these strains were never eliminated from lungs. ATCC 35767 was rapidly decreased and undetectable in lungs, spleens and livers within 16 weeks of infection. Overall, the clinical isolates other than strain 198 exhibited limited histological lesions with transient inflammatory changes in lungs 4 weeks after the inoculation, and thereafter the inflammation subsided at 16 weeks.

Table 3
Growth rate of MAC in THP-1 cells.

strain	Ratio of CFUs at[a]	
	Day 2	Day 7
33	0.29 ± 0.12	0.25 ± 0.16
198	18 ± 12*	1.30 ± 0.68*
288	0.47 ± 0.26	0.097 ± 0.055
27	0.54 ± 0.37	0.28 ± 0.11
36	2.4 ± 1.2	0.31 ± 0.11
347	1.1 ± 0.49	0.36 ± 0.23
25291	0.16 ± 0.048	0.11 ± 0.038
35767	0.059 ± 0.029	0.0070 ± 0.0048

* Significantly different ($P < 0.0001$) from values for any other strains studied as calculated by Scheffé's test.
[a] Means ± standard deviations of the ratio of CFUs to those at day 0.

3. Discussion

Virulence is defined as the quantitative ability of an agent to cause disease. The virulence of mycobacteria can be evaluated by the infection to macrophages and animals [17]. This is the first study that examined the virulence of MAC isolates from immunocompetent patients with different types of disease outcome. We found that strain 198, which derived from a patient with most serious disease, revealed high bacterial load both in THP-1 cells and in C57BL/6 mice among isolates studied. Strain-specific virulence of MAC has been implicated by some previous studies of the serovar 4 *M. avium* isolated from patients. In AIDS-related MAC disease, a serovar 4 *M. avium* isolate has shown to be one of the frequently isolated type [13], and a previous analysis of a serovar 4 isolate and ATCC strain has shown the superior virulence of serovar 4 *M. avium* in human macrophages [14]. In non-AIDS pulmonary MAC disease, our recent prospective study indicates that patients infected with serovar 4 *M. avium* has poorer prognosis than those infected with MAC of other serovars [16]; however, to our best knowledge, no study has shown the direct data of mycobacterial virulence of clinical isolates and clinical disease outcome. Strain 198 is the first MAC isolate whose experimental virulence corresponds to the serious disease outcome in humans. Thus, strain 198 has strain-specific strong virulence for immunocompetent humans and mice. We consider that strain 198 is worth further genetic investigation of virulence factors.

MAC strains hypervirulent for mice has been isolated previously by Pedrosa et al. including ATCC 25291 and MAC 101, which proliferate profoundly in mouse macrophages and in mice *in vivo* [12]. In this study, strain 198 proliferated in human macrophages, in correspondence with rapid clinical disease progression and additionally in mouse lungs. The consistency between experimental virulence in human cells and clinical disease outcome suggests that the capability of inducing such strong pathogenesis may be attributed mostly to the characteristics of the pathogen, i.e. virulence factor(s) for mammalian cells unique to strain 198. Previously Birkness et al. has shown the strong cytotoxic effect and growth of serovar 4 *M. avium* isolated from an AIDS patient in blood mononuclear cell-derived human macrophages compared with a serovar 2 strain from chickens (ATCC 35713). Therefore, we evaluated cytotoxicity of MAC strains by the microscopic morphology and by the LDH release from infected THP-1 cells; however, contrary to the expectation, strain 198 was not cytotoxic to THP-1. In addition, the release of LDH was lower in strain 33, ATCC 25291, and ATCC 35767 than in the previous experiment of *M. tuberculosis* infection to THP-1 cells (cytotoxicity in cases of *M. tuberculosis* H37Rv and H37Ra; approximately 30%) [18]. We assume that cytotoxic effect may not play a major role in displaying the virulence of MAC during infection, suggested by the similar result by Huttunen et al. showing the lack of cytotoxic effect of MAC in human 28SC macrophage and A549 lung epithelial cell lines evaluated by 3-(4,5-dimethyl-2-thiazolyl)-2,5-diphenyl-2H tetrazolium bromide (MTT) assay [19]. We speculate the virulence of strain 198 depends on the ability to survive or proliferate in macrophages rather than cytotoxic effect, which, may be causative for severe pulmonary MAC disease with rapid disease progression within a few years.

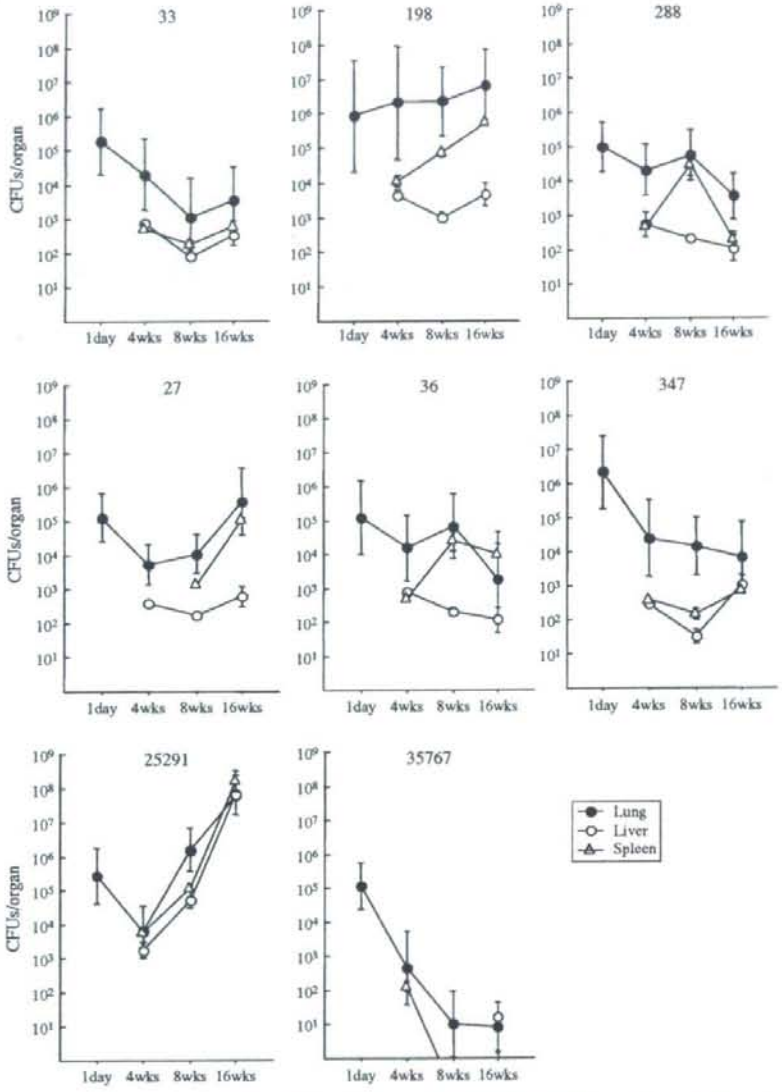

Fig. 1. Time course of mycobacterial growth in lungs, spleens and livers of C57BL/6 mice. Bacterial suspensions containing 1×10^5 CFUs were inoculated intratracheally to female C57BL/6 mice at the age of 7 weeks ($n = 20$ per strain). The lungs, livers and spleens of 5 mice per strain were sectioned at day 1 (only lungs), 4, 8, and 16 weeks later from challenge Data were presented as means ± standard deviations of CFUs/organ.

In this study, strain 198 showed strong virulence for mice at 16 weeks of infection similar to ATCC 25291; however, virulence for THP-1 cells was quite different, and pathogenic effects for mice within 4 weeks of infection was dissimilar between these two strains. These differences can be explained by the difference of immune response between host species and by the difference of immune phase. First, strain 198 could proliferate, but ATCC 25291 was rapidly eliminated in THP-1 cells (Table 3). In mouse macrophages mycobactericidal activity is attributed to nitric oxide produced by inducible nitric oxide synthase [20], whereas in human macrophages, it is attributed to Toll-like receptor signaling-dependent production of anti-microbial peptides [21,22]. Strain 198 is capable of proliferating under these two patterns of mycobactericidal activities, which suggests that strain 198 may have some virulence factors advantageous to survive both in human and mouse macrophages against mycobactericidal activity of the hosts, in contrast to ATCC 25291 which may lack virulence factors to survive in human macrophages. Second, strain 198 showed high bacterial load in lungs continuingly during 16 weeks of infection in mice, while ATCC 25291 proliferated after initial reduction in lungs at 4 weeks of infection (Fig. 1). The *in vitro* infection model using cell lines and the *in vivo* infection model using mice within 4 weeks reflects early stages of infection; on the other hand, the *in vivo* model after 8 weeks reflects chronic phase of infection [17,23]. The difference of pathogenic effects for mice within 4 weeks of infection suggests that strain 198 may resist both innate and acquired immunity, while ATCC 25291 may resist acquired immunity only. We assume that strain 198 and ATCC 25291 may possess different virulence mechanisms to persist in *in vivo* after development of acquired immunity.

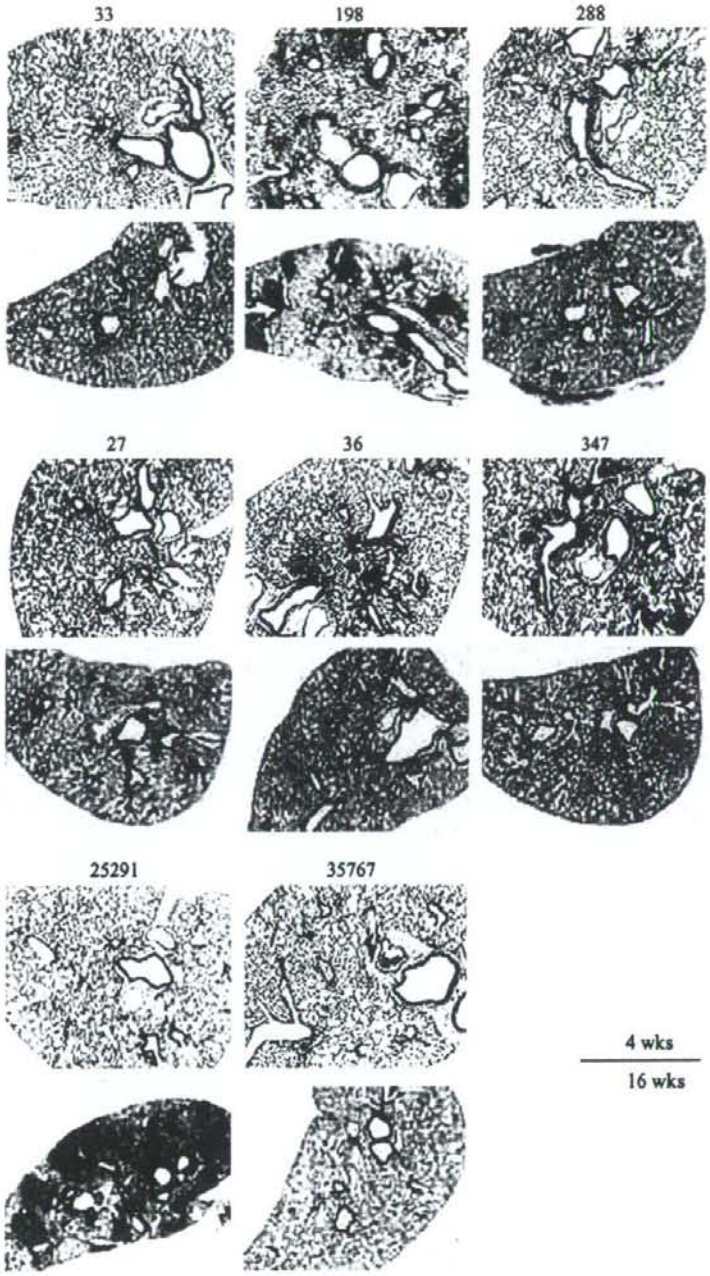

Fig. 2. Histological pictures of the lungs during 4 weeks or 16 weeks of infection in C57BL/6 mice by hematoxylin–eosin staining. Magnification, ×40.

In this study, clinical strains except for strain 198 did not show consistent virulence-associated phenotype among THP-1 cells, C57BL/6 mice, and clinical disease outcome. Similarly, Pedrosa et al. has also revealed that the growth of MAC in bone-marrow derived macrophages does not necessarily predict the virulence in mice by comparing the growth of 41 MAC isolates from various derives including humans, animals, and environment [12]. Although some clinical cases of pulmonary MAC disease may be caused by hyper-virulent strains such as strain 198, these findings of clinical and natural isolates suggest that virulence may not the only determinant of the pathogenesis of pulmonary MAC disease in the majority of clinical cases. The development of pulmonary MAC disease depends on the balance between bacterial virulence and host defense. It is widely accepted that patients with pulmonary MAC disease have some characteristics of clinical background, such as males in their 40s and early 50s who have a history of cigarette smoking and excessive alcohol use, and such as postmenopausal, nonsmoking females [3], and these patient characteristics might

possibly indicate unknown predisposing conditions which enhance susceptibility for pulmonary MAC infection. The diverse phenotype of clinical MAC strains may be attributed to the disease susceptibility of the hosts. We propose that pathogenic mechanism of human pulmonary MAC disease include two patterns; one is that the strong virulence of MAC strains such as strain 198 induces rapid mycobacterial growth and serious disease outcome, and the other is that relatively weak to moderate virulence interacts with predisposing conditions of the host, leading the wide range of clinical outcome.

This study was preliminary in that we did not identify the mechanism of hypervirulence of strain 198. We observed the consistency between hypervirulence in human macrophages bedsides in immunocompetent mice and severe clinical outcome only in strain 198, not in any other isolates studied. From this finding, we speculate the existence of strain-specific virulence factors of strain 198. Recent exponential advances have enabled whole genome sequence of two *M. avium* strains, *M. avium* 104 and *M. avium* subsp. *paratuberculosis* K-10. Based on these exhaustive information, comparative genomics of MAC organisms has revealed the different genomic components regarding virulence factors, such as *ser2* encoding glycosylation enzyme of the lipopeptide core to generate the glycopeptidolipids, mammalian cell entry (*mce*) gene homologs, and PE/PPE genes (i.e., with Pro Glu and Pro Pro Glu motifs) [24]. In addition, there are large sequence polymorphisms among MAC organisms, suggesting a large corresponding diversity in virulence [11,24]. We speculate that the virulence of MAC strains including strain 198 may be determined by insertion or deletion of virulence genes encoding known [24] or unknown virulence factors.

In summary, we demonstrated that certain clinical strain derived from patients of the progressive pulmonary MAC disease exhibits strong virulence in human macrophages and in immunocompetent mice. Among clinical isolates, strain 198 is the first isolate hypervirulent to both human macrophages and mice. Our data suggest that strain-to-strain differences in virulence may play a significant role in disease progression in humans. Although Sarmento et al. showed that capability of TNF-α production from macrophages inversely correlates with the virulence of MAC strains [25], we could not find such relationship among the isolates (data not shown). In future studies, we will identify the virulence/pathogenicity-associated factor(s) of strain 198 and survey the frequency of strain variation in immunocompetent patients with pulmonary MAC disease.

4. Materials and methods

4.1. Bacterial strains

We used six clinical isolates from non-AIDS patients with pulmonary MAC disease and two laboratory strains, *M. avium* ATCC 25291 (serovar 2) and *M. avium* ATCC 35767 (serovar 4), in this study. Clinical isolates were obtained between September and November in 2003 at Toneyama National Hospital. Informed consent was obtained from all patients according to the guideline of Institutional Review Board of Toneyama National Hospital. Diagnosis of pulmonary MAC disease was made according to the American Thoracic Society guideline [3]. The samples were derived from two groups of patients; one group exhibited progressive disease in spite of the combination chemotherapy including clarithromycin, ethambutol and rifampin recommended by the American Thoracic Society guideline (progressive type) [3], the other displayed no exacerbation without anti-microbial chemotherapy for approximately ten years or more (silent type). These types were determined by the laboratory findings at the period of sputum sampling (including sputum smear and culture, chest X-ray findings, and erythrocyte sedimentation rate) and the rapidness of disease progression (Table 1). Sputum specimens were mixed with 2% sodium hydroxide, and *N*-acetyl-L-cysteine and then centrifuged for 15 min at 3000 *g*. The supernatants were discarded, and the sediment was mixed at 1:10 (vol/vol) with sterile water. The bacteria were cultivated in Middlebrook 7H9 broth supplemented with albumin–dextrose–catalase, 0.02% glycerin and 0.05% Tween 80, and then kept at −80 °C until following experiments. Identification of MAC was made by polymerase chain reaction using a commercially available kit (AMPLICOR Mycobacterium Tuberculosis Test, Roche, Basel, Switzerland). The serovars of clinical isolates were identified by the liquid chromatography/mass spectrometry as described previously [26]. Strains not containing serovar-specific oligosaccharides were defined as apolar type.

4.2. Growth in 7H9 broth

Bacterial suspension was adjusted to be 0.2 by optical density (OD) at 630 nm. The samples were cultured in 5 ml of 7H9 media in plastic tubes without agitation After vortexing to dissolve aggregates, cultivated bacterial suspensions were inoculated at days 1, 3, and 5 by serial 10-fold dilutions on Middlebrook 7H11 agar plates supplemented with oleic acid–albumin–dextrose–catalase, and 0.05% glycerol (7H11-OADC) agar plates in triplicate. The number of CFUs was counted after cultivating at 37 °C for 3 weeks.

4.3. Infection of THP-1 cells with MAC in vitro

THP-1 cells were purchased from Health Science Research Resources Bank (Tokyo, Japan). The cells were cultured in RPMI1640 containing 10% heat-inactivated fetal bovine serum (FBS; Equitech-bio, TX), and subcultured every 3–4 days. THP-1 cells were differentiated by 100 nM PMA (Sigma–Aldrich, St Louis, MO) for 48 h before infection. Before 48 h of infection, 1 ml of 2×10^5/ml cells was cultured in RPMI1640 containing 5% human serum (AB-blood group) in 24-well plates. Then, 1 ml of 2×10^4 CFUs/ml bacteria was exposed to the cultured cells for 24 h without opsonization (multiplicity of infection; 0.1 bacteria/cell). After that, the cells were treated with 20 μg/ml of gentamicin for 3 h to kill extracellular bacteria, followed by washing 4 times by RPMI1640. The infected cells were cultured in 2 ml of RPMI1640 containing 5% human serum. At days 0 and 7, uninfected bacteria were removed by washing with RPMI1640 4 times, and 500 μl of filter-sterilized phosphate buffered saline containing 0.5% Triton X-100 (Wako, Osaka, Japan) was treated per well to lyse cell membrane. The intracellular survival of bacteria was determined by counting CFUs by inoculating the cell lysate on 7H11-OADC agar plates. The experiment was performed in triplicate.

4.4. Assays for cytotoxicity

Cytotoxic effects were evaluated by the release of LDH from the cells. LDH activity of culture supernatants was determined by a commercially available kit (Roche, Basel, Switzerland). Supernatants were diluted to be 10^{-1} by distilled water for optimal reaction. The diluents were reacted with reaction mixture for 30 min, and then the OD was measured at 492 nm. Supernatants of completely lysed uninfected cells with filter-sterilized phosphate buffered saline containing 20% Triton X-100 and those of uninfected cells untreated with Triton X-100 were served as high and low controls, respectively. Cytotoxicity (%) was calculated as follows; $(OD_{sample} - OD_{low\ control}) \times 100/(OD_{high\ control} - OD_{low\ control})$. The measurement was performed in triplicate.